Cooling and exhumation of the Western Betic Cordilleras, $^{40}Ar/^{39}Ar$ thermochronological constraints on a collapsed terrane

P. Monié [a], R.L. Torres-Roldán [b], A. García-Casco [b]

[a] *Laboratoire de Tectonique et Géochronologie, URA CNRS 1371, USTL, Place E. Bataillon, 34095 Montpellier Cédex, France*
[b] *Departamento de Mineralogía y Petrología and Instituto Andaluz de Geología Mediterranea, CSIC- Universidad de Granada, Fuentenueva s/n, 18002 Granada, Spain*

Abstract

New $^{40}Ar/^{39}Ar$ data on amphiboles, muscovites, biotites and potassium-feldspars from different tectono-metamorphic units of the Western Alpujarrides (Betic Cordilleras, southern Spain) help to constrain the $P-T-t$ evolution of this Alpine collisional belt. During an initial stage of plate convergence between Africa and Eurasia, the Alpujarride metamorphic rocks evolved along increasing pressure–temperature paths, locally reaching eclogitic conditions, but the timing of peak metamorphism is only constrained to be earlier than 25 Ma. In the interval of 25–22 Ma, the Alpujarride rocks underwent strong adiabatic decompression related to the collapse of the previously thickened crust. We propose that the main phase of synmetamorphic ductile deformation and thinning of the metamorphic pile was related to this extensional event. The last step is marked by fast cooling of the hot Alpujarride rocks below 600°C, resulting in a striking convergence of our $^{40}Ar/^{39}Ar$ determinations in the range 19–20 Ma. Cooling rates in the range 100–350°C/m.y. are indicated for this period, associated with exhumation rates of less than 3 km/m.y. We suggest that fast cooling took place primarily as a result of thermal relaxation of the abnormally steep geotherm resulting from extensional tectonics which has the effect of juxtaposing thinned rock bodies with contrasting temperatures along shear zones and faults. The main implication of this data set is that the Western Alpujarrides present a structural and metamorphic development which should be regarded as characteristic of "collapsed terranes".

1. Introduction

During recent years, metamorphic belts have been subjected to routine thermochronological $^{40}Ar/^{39}Ar$ studies aimed at unravelling their cooling histories and deciphering structural relationships between their constitutive units. By determining closure temperatures of the various minerals used as thermochronometers, it is possible to reconstruct the cooling path of a given area over temperatures ranging from 150° to > 550°C (e.g. McDougall and Harrison, 1988; Hurford et al., 1989). This temperature range can be extended from 100 to 750°C by parallel investigations using U–Pb, Sm–Nd, Rb–Sr and fission track methods. Furthermore, if peak-metamor-

phic conditions and P–T paths are well-known, then the integration of thermochronological and petrological results can yield important constraints on exhumation rates. In addition, post-metamorphic sedimentary formations containing metamorphic clasts place important constraints on cooling and exhumation models. The comparison between the palaeostratigraphic age of the sediments, which constitutes a minimum age for the aerial exposure of the enclosed metamorphic pebbles, and the time at which the clastic minerals cooled below their closure temperatures for argon diffusion may allow extrapolation of P–T–t paths towards surface conditions.

In this paper, $^{40}Ar/^{39}Ar$ age spectra for micas, amphiboles and feldspars from rocks belonging to several Alpujarride units in the western internal zone of the Betic Cordilleras (southern Spain) are presented. During the Alpine orogeny, the African plate collided with the European plate to form the various Alpine chains of the Western Mediterranean (e.g. Coward and Dietrich, 1989). The Betic belt (Fig. 1), together with its African counterpart in the Moroccan Rif, represents the western termination of these chains in Europe, and has been the locus of a protracted tectonic, metamorphic and magmatic history in Mesozoic and Cenozoic times (cf. Torres-Roldán, 1979, and references therein).

The geology of the Betic Cordilleras (see Fontboté and Vera, 1986, for a recent review) can be divided into a foreland domain made mostly of unmetamorphosed Mesozoic and Tertiary sedimentary rocks (the Prebetic and Subbetic zones) and an internal domain (the Betic Zone) that consists of three main nappe ensembles, i.e., from top to bottom, the Malaguides, the Alpujarrides and the Nevado–Filabrides. A Palaeozoic basement and a (Permian–)Triassic, Mesozoic and Tertiary cover are well identified in the Malaguides (e.g. Mäkel, 1985), most of which show little evidence of Alpine metamorphic overprint. The underlying Alpujarrides and Nevado–Filabrides both consist of a Palaeozoic (or older) basement and a (Permian–)Triassic pelitic and carbonatic cover (see Diaz de Federico et al., 1990, for a review) and both underwent Alpine high-pressure metamorphism and subsequent

evolution and retrogression along variable P–T paths. Eclogites and other high-pressure low-temperature (HP/LT) rocks have been known for some time within the Nevado–Filabrides (Nijhuis, 1964; Puga, 1977) and various trajectories have been proposed for their exhumation (e.g. Gómez-Pugnaire and Fernández-Soler, 1987; Bakker et al., 1989; Puga et al., 1989), but time markers are very scarce (Monié et al., 1991; De Jong et al., 1992). In the Alpujarrides, HP/LT carpholite-bearing relict assemblages are preserved in low-grade pelitic rocks within several units of the Central and Western Betic Zones (Goffé et al., 1989; Azañón and Goffé, 1991), and a relict eclogitic assemblage has also been reported recently in a layer beneath the Ronda peridotites (Tubía and Gil Ibarguchi, 1991), all giving evidence for an early burial at 35–50 km depth during a period of crustal thickening. Petrological studies indicate that this HP/LT event was succeeded by thermal reequilibration under HP/HT conditions, which in turn was followed by decompression along a nearly isothermal path and final exhumation and cooling (e.g. Westerhof, 1977; Torres-Roldán, 1981; García-Casco et al., 1993).

The mechanism by which such deep-seated rocks were transported to the surface is a problem currently debated in all collisional belts. In the Betics, an additional problem arises concerning the crustal emplacement of the Ronda peridotites and its bearing on the metamorphic evolution of the enclosing Alpujarride sequences. Reconstruction of P–T–t paths offers an opportunity to further constrain the nature of the tectonic processes involved in the exhumation of the Betic rocks. Preliminary $^{40}Ar/^{39}Ar$ results on HP/LT metamorphic assemblages have been reported in an earlier paper (Monié et al., 1991). Here we present a series of new $^{40}Ar/^{39}Ar$ age determinations on rocks which experienced higher-grade (amphibolite to granulite facies) conditions in different Alpujarride units of the Western Betic Zone, including metamorphic pebbles from a nappe-sealing sedimentary formation (the Viñuela formation, Boulin et al., 1973). The new ages are consistent with available radiometric and palaeostratigraphic constraints and sug-

gest very high rates of cooling and uplift related to late-metamorphic extensional tectonics in the area.

2. Geological setting of the Western Alpujarrides

2.1. Geology

The Western Betic Zone, as used in this report, refers to the westernmost segment of the internal zone of the Betic Cordilleras and includes essentially three regions, i.e., from west to east, the southern Serranía de Ronda, the Montes de Málaga and the Vélez Málaga–Sierra Tejeda Massif (Fig. 1). All three regions contain a number of tectonic units belonging to the Alpujarride and Malaguide ensembles, although Malaguide outcrops make the bulk of the Montes de Málaga (the type locality) and Alpujarride sequences predominate in the other two regions. Within the Alpujarrides, two main groups of units can be distinguished on the basis of lithological variations, relative structural position and metamorphic development: the Casares–Los Reales Group and the Blanca Group (see also Martín-Algarra, 1987; Balanyá and García-Dueñas, 1991). In most instances, the units of the Casares–Los Reales Group lie directly beneath the Malaguide sequences and are in turn underlain by those of the Blanca Group. Stratigraphic repetitions across the contacts suggest that these consisted of early overthrusts. In many instances, however, the existence of discontinuities (omissions) of metamorphic grade indicate that many of the present contacts represent extensional faults, rather than the original thrust boundaries (García-Dueñas and Balanyá, 1991).

In the southern Serranía de Ronda, a number of large orogenic lherzolite bodies, often collectively referred to as the Ronda peridotites, appear at the bottom of the metamorphic sequence of the Casares–Los Reales units, typically next to high-grade pelitic granulites and gneisses that grade upwards into progressively lower-grade metapelites and marbles (Loomis, 1972; Torres-Roldán, 1981). The age and stratigraphic relationships of this "primary" crustal envelope of

the peridotites are mostly unknown, but on the basis of lithologic comparisons with the palaeontologically better constrained Malaguide sequences, it probably consists of Palaeozoic or older basement and Permian–Triassic cover rocks. The stratigraphic column of the underlying Blanca units resembles that of the Casares–Los Reales units, although the fragmented nature of outcrops makes its reconstruction more difficult. It is noteworthy that, in contrast with the low- to medium-grade assemblages of the overlying Permian–Triassic rocks of the Casares–Los Reales units, the probably correlative Triassic rocks of the Blanca units commonly consist of high-grade marbles interlayered with anatectic gneisses, consistent with their deeper location in the nappe pile during metamorphism. The latter also contain interlayered metabasites, which are rare or absent in the Triassic of the Casares–Los Reales units.

In the Vélez Málaga–Sierra Tejeda Massif, peridotite outcrops are lacking, but a similar grouping of existing Alpujarride units can be made using the same criteria as in the southern Serranía de Ronda (Fig. 1). The Casares–Los Reales Group is represented by the uppermost tectonic unit, locally referred to as the Torrox unit (García-Casco et al., 1993), and the Blanca Group by the Sierra Tejeda and Cómpeta units (from top to bottom; undifferentiated in Fig. 1), whose outcrops form the core of the massif and tectonically underlie the Torrox unit. The Permian–Triassic sequence of the Torrox unit reached only low-grade conditions, whereas the same sequences in the underlying Sierra Tejeda and Cómpeta units bear medium- to high-grade assemblages. This supports the proposed tectonic correlation with the groups distinguished in the southern Serranía de Ronda, in spite of the absence of the deeper granulite-facies sections and associated ultramafic basement in the Torrox unit. However, the presence of a marked positive gravity anomaly to the south of Torrox (Bonini et al., 1973) suggests that this ultramafic basement may be present at depth, hidden by the occurrence of late-extensional faulting. In the Torrox unit, small bodies of leucocratic gneisses appear within the graphitic schists that compose the bulk of the
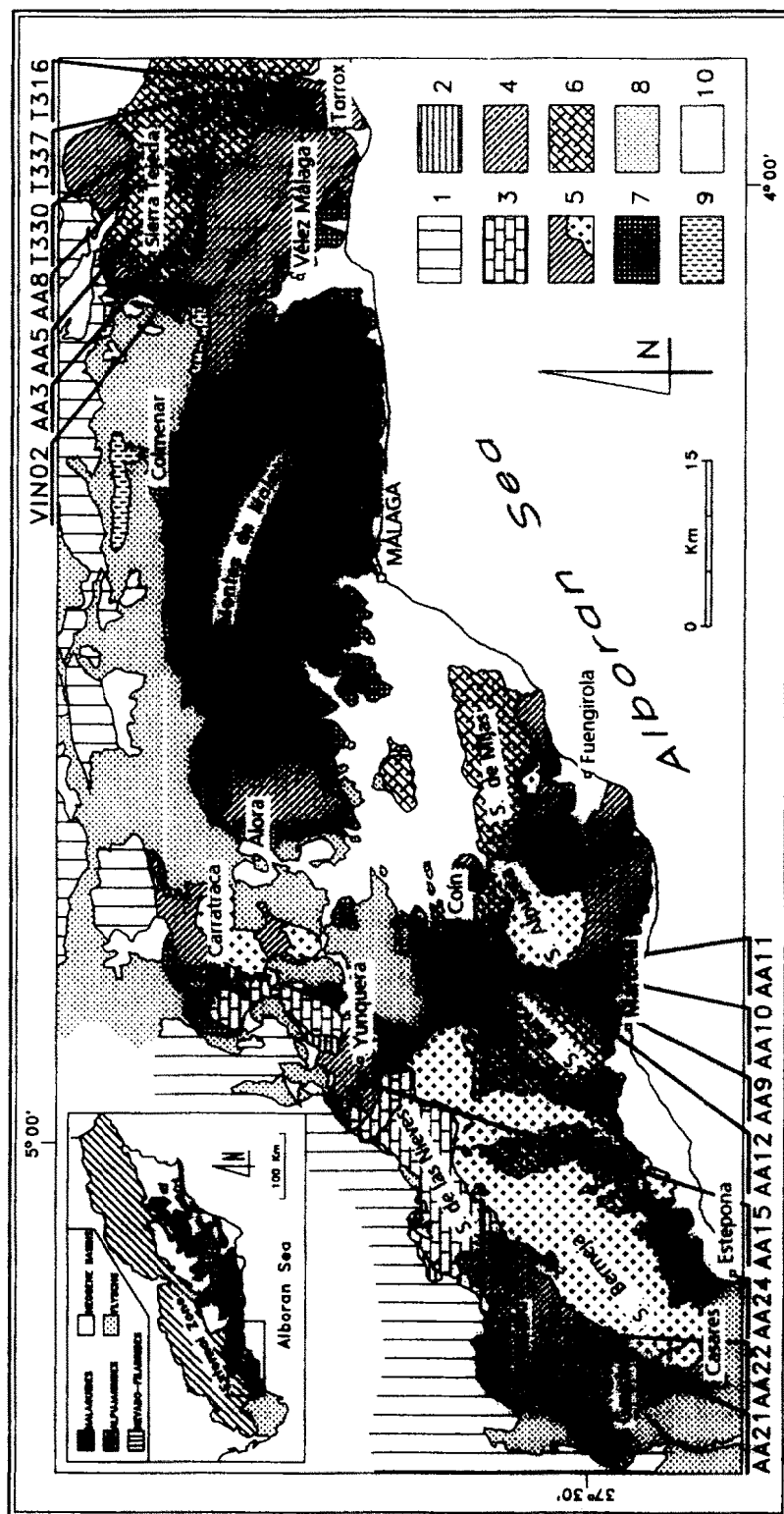
Fig. 1. Geological sketch map of the Western Betic Cordilleras, including the location of the samples: *1* = external zones; *2* = Betic Dorsal; *3* = Nieves unit; *4* and *5* = type Casares–Los Reales units (*4* = Yunquera), including peridotites (cross ornamentation); *6* = type Blanca units; *7* = Malaguide units; *8* = Early Cretaceous to Early Miocene flysch; *9* = Miocene syn-tectonic deposits (type Viñuela); *10* = Neogene and Quaternary deposits (post-tectonic). The tectonic contacts are undifferentiated since controversial opinions still exist concerning their nature and geometry.

Palaeozoic basement. The best known of these is located near the village of Torrox.

2.2. Metamorphic evolution

The $P-T$ paths in Fig. 2 document a three-stage metamorphic evolution for the crustal portions of the Alpujarride units. Sparse relict eclogitic assemblages in metabasites (Tubía and Gil Ibarguchi, 1991) and carpholite-bearing assemblages in metapelites (Goffé et al., 1989; Azanón and Goffé, 1991) indicate that high P/T-ratio metamorphic gradients characterized the initial phase of Alpine metamorphism, at least in previously unmetamorphosed Permian–Triassic cover sequences. Intermediate P/T-ratio conditions followed this initial stage, as recorded by peak temperatures in excess of 800°C in K-feldspar–kyanite–garnet and pyroxene–garnet–plagioclase assemblages in high-pressure (8–13 kbar) pelitic and mafic granulites near the contacts with the peridotite bodies (Loomis, 1972; Kornprobst, 1974; Westerhof, 1977; Torres-Roldán, 1981, and unpublished data). Intermediate P/T ratios also characterize peak metamorphism at shallower structural levels (García-Casco et al., 1992, 1993; Fig. 2). During the third stage, low P/T-ratio assemblages overprinted the earlier intermediate P/T-ratio assemblages, as evidenced by cordierite coronas around garnet and inversion of kyanite to sillimanite in pelitic granulites (Loomis, 1976), amphibolitization of early eclogitic assemblages (Tubía and Gil Ibarguchi, 1991) and by cordierite–andalusite assemblages in the lower-grade metapelites (Torres-Roldán, 1981; García-Casco et al., 1992). The degree of replacement of the preexisting higher P/T-ratio assemblages varies widely, mostly as a function of local kinetic constraints, but replacement is generally more complete in the deeper type Blanca units. That only partial reequilibration had taken place during late, low P/T-ratio metamorphism, even in high-grade rocks, is compatible with the high rates of cooling discussed below.

The orogenic lherzolite sheets located at the base of the Casares–Los Reales units also show complex metamorphic relationships (cf. Obata, 1980) that have been variously interpreted (see
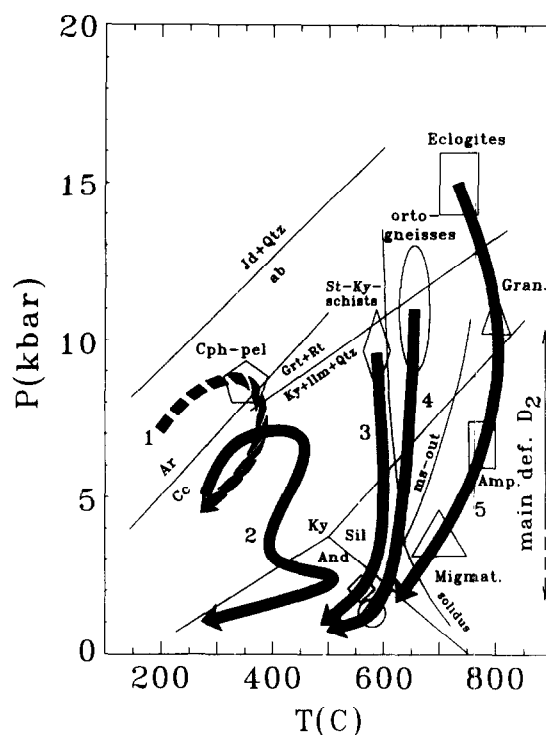

Fig. 2. $P-T$ diagram showing selected phase equilibria and $P-T$ paths (numbers) for several Alpujarride units: $1 =$ tentative $P-T$ path for carpholite-bearing pelites in Trevenque-type units (after Goffé et al., 1989); $2 = P-T$ path for the Almanzora unit in the Eastern Betic Zone (after Bakker et al., 1989); $3 = P-T$ path for St + Bt + Grt + Ky + Fib + And graphitic schists in the Torrox unit (unpublished data); $4 = P-T$ path for the Torrox anatectic leucogneisses (after García-Casco et al., 1993); $5 = P-T$ path for high-grade rocks (boxes = mafic rocks, triangles = felsic and metapelitic rocks, Gran. = granulites, Amph. = amphibolites, Migmat. = migmatites) in the Blanca unit (compilation after Westerhof, 1977; Torres-Roldán, 1981; Tubía and Gil Ibarguchi, 1991). Sources of phase equilibria: Al_2SiO_5 triple point after Holdaway (1971); the granite solidus and ms-out reactions after Thompson (1982); jadeite + quartz = albite after Newton and Kennedy (1968); aragonite = calcite after Boettcher and Wyllie (1988); garnet + rutile = kyanite + ilmenite + quartz after Bohlen et al. (1983). The development of the main deformation (labelled D_2) occurred during the decompression of the metamorphic sequences, as indicated by the right-hand vertical line.

also Saddiqi et al., 1988, and Van der Wal, 1993). A discussion concerning these relationships is beyond the scope of this paper. Nonetheless, the persistence of marked disequilibrium in these high-temperature massives is compatible with the

metamorphic history outlined for their crustal envelopes, particularly in their failure to reequilibrate at low pressure before final cooling.

2.3. Tectonic development

Diverse competing tectonic interpretations have been proposed for the evolution of the Western Alpujarrides (Torres-Roldán, 1979; Tubía and Cuevas, 1986; Platt and Vissers, 1989; Doblas and Oyarzun, 1990; Tubía et al., 1992). However, the nature of tectonic events accompanying their metamorphic evolution is poorly constrained, especially the earlier pre- and syn-metamorphic events whose kinematic indicators have been largely destroyed during the late syn-decompressional tectonic development related to exhumation of crustal and mantle rocks in this area. Clues to the nature of the earlier tectonic events involved in the Alpine orogeny can nonetheless be inferred from the evolution of metamorphism, as well as from observations on crustal development and plate kinematics. These are all compatible with the occurrence of a major post-Cretaceous continental collision, which reached its climax in Late Eocene to Middle Oligocene times. The collision led to the stacking of crustal segments now represented by the two groups of Alpujarride units and the overlying Malaguides. In the case of the Casares–Los Reales segment, a slice of underlying upper-mantle material was also involved in the stack. Considerable crustal thickening after collision is witnessed by the fact that pressures in the range of 10–12 kbar were attained in crustal rocks from the intermediate Casares–Los Reales segment and as high as 16–17 kbar in the underlying Blanca segment (Sect. 2.2). Thickening culminated in the Late Oligocene (Monié et al., 1991) which marks the beginning of extensional tectonics, with important extensional detachments taking place up to the Middle Miocene (cf. García-Dueñas and Balanyá, 1991). At depth, early extension took place at high temperatures, including the development of the main foliation with kinematic indicators suggesting an east-northeast direction of movement (Tubía and Cuevas, 1986). The late stages of development of

this foliation are demonstrably coeval with mineral reactions yielding low-pressure assemblages (Torres-Roldán, 1981; García-Casco et al., 1993). Early extension also resulted in pronounced distributed thinning of the individual Alpujarride sequences, allowing the buried rocks to turn back to higher crustal levels along the isothermal paths illustrated in Fig. 2. The end of this early extension is marked by the intrusion of 22–23 Ma old tholeiitic to calc-alkaline E–W-trending dykes that postdate the main foliation (Torres-Roldán et al., 1986). It is noteworthy that ongoing extension in the Alboran centre was coeval, to the west, with overthrusting of the internal zones over the foreland domain along the Gibraltar arc frontal thrust (García-Dueñas et al., 1992), which may have influenced the cooling history of the overthrusted margin of the Alboran domain (see below).

2.4. Previous geochronological data

In an early work, Loomis (1975) reported K–Ar whole-rock and biotite ages from the gneisses in contact with the Alpujata and Bermeja peridotites ranging from about 22 to 81 Ma. Subsequent investigation via the $^{40}Ar/^{39}Ar$ technique revealed that an excess argon component preferentially held in cordierite was responsible for this age scatter, and accordingly, the 22 Ma ages of cordierite-free samples represent reasonable cooling ages (Seideman, 1976). Both Rb–Sr and K–Ar dates on biotites from the contact rocks with the Alpujata peridotites have been obtained that support an age of 19.3 ± 0.6 Ma for cooling to a temperature of about 300°C, the closure temperature for Ar and Sr in biotite (Priem et al., 1979). Only one biotite from the contact with the Bermeja peridotites yielded an older age of 21.1 ± 0.6 Ma, suggesting a possible diachronism in the cooling/uplift history of the Western Alpujarrides. Note that biotites from the structurally equivalent Sebtide units above the Beni Bousera peridotites in the Moroccan Rif yielded K–Ar ages of about 22 Ma that seem to support this diachronism (Michard et al., 1983, 1991). Since these pioneering works, additional data on meta-

morphic rocks have been obtained recently using Rb–Sr and $^{40}Ar/^{39}Ar$ geochronology. A Rb–Sr date of 21 ± 2 Ma based on four whole-rock muscovite pairs has been reported for the end of Alpine ductile deformation (Zeck et al., 1989), whereas muscovites and biotites yield $^{40}Ar/^{39}Ar$ plateau ages (Monié et al., 1991; Zeck et al., 1992) which are indistinguishable from the K–Ar ages reported by Priem et al. (1979). A single $^{40}Ar/^{39}Ar$ release spectrum on a Si-rich phengite from a carpholite-bearing HP/LT assemblage may date the end of high-pressure metamorphism and crustal thickening at 25 Ma (Monié et al., 1991). A 22 Ma age is proposed for the emplacement of peridotites at high crustal levels (Priem et al., 1979; Zindler et al., 1983; Reisberg et al., 1989). Recent Pb–Nd isotope systematics on pyroxenites suggest that the initial ascent of the Ronda peridotites from deep levels (> 150 km) could be the result of a Jurassic extensional episode (Pearson et al., 1993).

As outlined above, the Alpujarrides clearly preserve a polyphase metamorphic history; yet it is difficult to infer more than one event on the basis of available geochronologic data. Furthermore, the narrow data set for this event suggests that the Alpujarrides experienced cooling rates up to 100–300°C/m.y. during the 22–19 Ma interval (Zeck et al., 1989, 1992).

3. Analytical method

Our experimental $^{40}Ar/^{39}Ar$ procedure is similar to that reported in the literature (e.g. McDougall and Harrison, 1988). Mineral concentrates were prepared from crushed and sieved rock powders using magnetic separator, heavy liquid and ultrasonic cleaning techniques. The minerals were encapsulated in evacuated quartz vials and irradiated with fast neutrons together with an intralaboratory hornblende flux monitor with an age of 344.5 ± 4 Ma. Two nuclear facilities have been used during this study, the Osiris reactor in Saclay and the Siloe reactor in Grenoble. Shielding by a 0.5 mm thick Cd-foil was applied to the samples irradiated in the Siloe reactor. The fast neutron fluence was approximately 1.5×10^{18} n cm^{-2}. KF and CaF$_2$ salts were irradiated in both reactors and the correction factors for interference reactions from K and Ca were as follows: $(^{36}Ar/^{37}Ar)_{Ca} = 2.93 \times 10^{-4}$, $(^{39}Ar/^{37}Ar)_{Ca} = 7.61 \times 10^{-4}$, $(^{40}Ar/^{39}Ar)_K = 1.92 \times 10^{-2}$ for the Osiris reactor; $(^{36}Ar/^{37}Ar)_{Ca} = 2.87 \times 10^{-4}$, $(^{39}Ar/^{37}Ar)_{Ca} = 7.08 \times 10^{-4}$ for the Siloe reactor. Minor interference from K-derived ^{40}Ar was found in Siloe due to the Cd shielding (McDougall and Harrison, 1988). After irradiation, the minerals were wrapped in Ni-foils and brought into a UHV glass extraction system, evacuated with ion and turbo pumps and connected to a highly modified THN 205E mass spectrometer. The minerals were pre-heated at 200°C for 24 h. From 400 to 900°C, the samples were stepwise heated in a quartz tube by a Kanthal resistance furnace. A W–Re thermocouple is located immediately adjacent to the sample, outside the quartz tube. A thermal gradient less than ± 5°C was independently measured between the outside and inside regions of the quartz tube. Above 900°C, heating was performed with a high-frequency inductor in a Mo crucible and temperature-monitoring was achieved by optical pyrometry. Gas clean-up was accomplished with cold traps and SAES getters. All data were corrected for mass discrimination, radioactive decay of ^{37}Ar and ^{39}Ar, isotopic interferences with Ca and K and blanks. System blanks ranged from 0.8×10^{-13} mol ^{40}Ar at 400°C up to 4.5×10^{-13} mol ^{40}Ar at 1500°C. The errors on single steps are 2σ. The J-error has been propagated only into the total-fusion and plateau ages. The decay constants are those of Steiger and Jäger (1977). $^{36}Ar/^{40}Ar$ vs. $^{39}Ar/^{40}Ar$ isotope correlation plots have been calculated using the regression method of York (1969). This construction yields two intercept values that correspond to the pure trapped and pure radiogenic components in the mineral (Roddick et al., 1980). Occasionally, more than one linear array may be observed, resulting from the presence of multiple argon reservoirs within the sample (Heizler and Harrison, 1988). Generally, the low-temperature heating steps exhibit scatter on isochron diagrams and have been excluded from the regression.

4. Results

As mentioned in the introduction, a typical Alpujarride sequence consists of metapelitic and carbonate Permian–Triassic cover and Palaeozoic or older basement dominated by graphitic schists

and metagreywackes. Each Alpujarride unit presents a more or less complete section of this type-sequence, with a metamorphic grade generally decreasing toward the cover. Due to late-metamorphic extension, continuous series of assemblages indicating a temperature range up to

Table 1

Summary of $^{40}Ar/^{39}Ar$ results in the Western Alpujarrides (samples from the Vélez Málaga–Sierra Tejeda Massif and from the Serranía de Ronda)

Sample	Lithology Location	Total date	Plateau or "near-plateau" date	Correlation date	Initial $^{40}Ar/^{36}Ar$ (MSWD)
AA3 Muscovite	Gneiss COMPETA	18.3 ± 0.3	18.3 ± 0.3	18.9 ± 0.4	277 ± 45 (0.07)
AA5 Muscovite	Metaquartzite SIERRA TEJEDA	18.6 ± 0.2	no plateau	18.9 ± 0.5	282 ± 35 (1.40)
AA8 Amphibole	Amphibolite SIERRA TEJEDA	19.4 ± 1.4	18.5 ± 0.8	18.9 ± 0.6	302 ± 31 (0.02)
T316 Biotite	Banded gneiss	12.9 ± 0.2	no plateau	–	–
T316 Muscovite	TORROX	19.0 ± 0.2	19.1 ± 0.2	19.2 ± 0.3	283 ± 35 (0.32)
T316 K-feldspar		22.3 ± 0.2	no plateau	19.8 ± 0.4 (LT)	505 ± 74 (1.05)
T330 Biotite	Pelitic gneiss	18.3 ± 0.2	18.5 ± 0.2	18.8 ± 0.6	281 ± 30 (0.07)
T330 Muscovite	TORROX	19.0 ± 0.2	19.1 ± 0.2	19.1 ± 0.8	302 ± 50 (0.47)
T337 Biotite	Leucocratic	19.2 ± 0.2	19.4 ± 0.2	20.2 ± 0.3	218 ± 21 (0.62)
T337 Muscovite	augengneiss	18.6 ± 0.2	18.8 ± 0.2	19.0 ± 0.7	296 ± 73 (0.96)
T337 K-feldspar	TORROX	23.6 ± 0.2	no plateau	19.6 ± 0.7 (LT)	306 ± 69 (0.35)
VIN02 Biotite	Graph. schist VIÑUELA	19.2 ± 0.4	21.9 ± 0.4	21.7 ± 0.6	307 ± 28 (0.23)
AA9 Amphibole	Amphibolite SIERRA BLANCA	18.9 ± 0.6	18.7 ± 0.6	19.1 ± 1.2	288 ± 51 (0.04)
AA11 Biotite	Granodiorite OJEN	18.7 ± 0.2	18.8 ± 0.2	19.3 ± 0.2	280 ± 25 (0.55)
AA10 Biotite	idem, mylonitic	20.2 ± 0.3	(integration of two identical step ages)		
AA15 Muscovite	Gneiss YUNQUERA	19.3 ± 0.3	19.4 ± 0.4	19.5 ± 0.6	292 ± 48 (0.20)
AA21 Biotite	Gneiss CASARES–LOS REALES	21.4 ± 0.3	21.3 ± 0.3	21.1 ± 0.2	308 ± 11 (0.10)
AA22 Biotite	Granulite CASARES–LOS REALES	21.6 ± 0.4	21.6 ± 0.4	21.6 ± 0.2	295 ± 9 (0.49)
AA24 Phlogopite	Marble SIERRA BLANCA	20.2 ± 0.2	20.2 ± 0.2	20.2 ± 0.3	299 ± 29 (0.12)

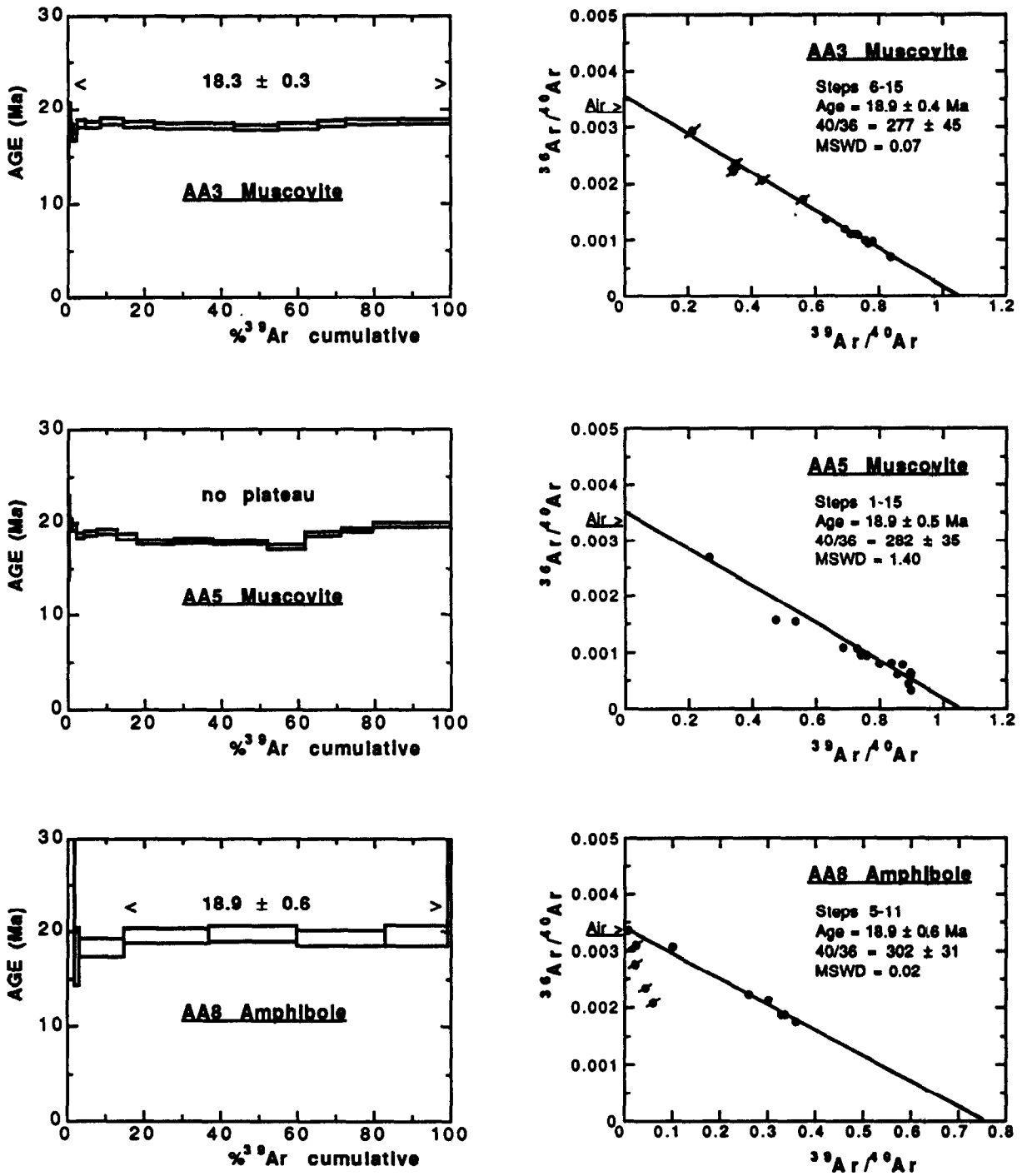|		$^{40}Ar_{rad}/^{39}Ar$	$^{40}Ar_{rad}$ (10^{-16} mol)	Age	$\%^{40}Ar_{atm}$
AA12 BIOTITE	Granulite	0.684	29.84	19.1 ± 0.3	1.40
	OJEN	0.680	10.99	19.0 + 0.5	7.21
Laser-probe fusion dating		0.600	21.92	16.8 ± 0.4	1.90

Fig. 3. Age spectra and isotope correlation plots for samples of the Sierra Tejeda Massif. Data points marked with a bar have been excluded from the regression.

several hundred degrees Celsius may be represented within fairly thin rock sequences (down to less than 1 km). Given the above remarks, and the possibility that different tectonic units followed distinct cooling paths, the sampling for this study was generally set up so as to: (1) include only amphibolite-facies or higher-grade rocks, equilibrated at temperatures high enough for complete radiogenic argon resetting, (2) represent most units, and (3) include, as far as possible, samples with minerals having different closure temperatures for Ar. Sampling localities are indicated in Fig. 1.

$^{40}Ar/^{39}Ar$ results from the Western Alpujarride samples are summarized in Table 1 and are presented as age spectra and isotope correlation plots. The majority of samples show nearly flat age spectra for a large percentage of the gas released, with plateau ages or "near-plateau" ages ranging from about 19 to 22 Ma. A "near-plateau" age does not strictly satisfy the definition of a plateau in the sense of Fleck et al. (1977) and shows internal age variations higher than the 2σ level. However, the corresponding gas fractions generally lie on a single mixing line in the isotope correlation plot and the age calculated from the $^{39}Ar/^{40}Ar$ intercept does not differ markedly from the "near-plateau" age. Spectra with internal age discordances were mainly obtained with samples showing a state of chemical and textural disequilibrium, reflecting their evolution from high-pressure to low-pressure conditions. Nonetheless, in a few cases, the initially trapped non-radiogenic argon component has a $^{40}Ar/^{36}Ar$ ratio significantly different from the present-day atmospheric value of 295.5 (e.g. T316 K-feldspar). For this reason, we assumed that the age defined by the correlation plot is the best estimate for the closure of the mineral (cf. Heizler and Harrison, 1988).

4.1. Vélez Málaga–Sierra Tejeda Massif

Thirteen minerals were analyzed from seven rocks collected at different structural levels of the metamorphic pile and results are presented in ascending structural order.

Sample AA3 is a coarse-grained, anatectic, two-mica gneiss interlayered with high-grade Triassic marbles of the Cómpeta unit (Blanca Group), the deepest tectonic element in the massif. Texture and mineral assemblage in this sample are very similar to those of sample T337, described in detail below, and a peak temperature of about 650°C is consistent with evidence of partial melting. The $^{40}Ar/^{39}Ar$ results of muscovite are shown in Fig. 3 and corresponds to an isochron date of 18.9 ± 0.4 Ma calculated on ten successive heating steps.

Samples AA5 and AA8 come from the lower part of the Permian–Triassic cover of the overlying Sierra Tejeda unit (Blanca Group) and consist respectively of a quartzitic biotite–muscovite schist and an amphibolite. Although none of these samples contains diagnostic assemblages, their location within a zone of staurolite–garnet–biotite–kyanite schists indicates peak temperatures in the range of 550–600°C. The age spectra and isochrons for muscovite and hornblende from these samples are reported in Fig. 3. The muscovite has a saddle-shaped spectrum with maximum and minimum ages of 19.8 and 17.8 Ma, respectively. Ca/K values are low but demonstrate a similar saddle-shaped variation during incremental heating. Tentatively, an isochron date of 18.9 ± 0.5 Ma has been calculated on the total gas released, but the scattering of the data points suggests that Ar was released from different reservoirs as illustrated by the Ca/K pattern. This interpretation is in line with petro-structural features indicating incomplete recrystallization of this quartzitic schist which preserves two generations of white mica and abundant high-pressure relict minerals. The hornblende exhibits a flat age pattern for 80% of gas released and an isochron date of 18.9 ± 0.6 Ma, corresponding to constant Ca/K values.

Micas and K-feldspars were analyzed from three samples of the Torrox gneiss complex, a heterogeneous gneissic body located towards the bottom of the Torrox unit (Casares–Los Reales Group), beneath a thick sequence of amphibolite-facies graphitic schists. These samples preserve a complex history of mineral growth and dissolution as discussed by García-Casco et al. (1993).

Sample T330 is from a band of metapelitic gneiss (lacking K-feldspar) surrounding the main gneiss body and providing a gradational transition between this body and the enclosing graphitic schists. These gneisses have mineral assemblages similar to those of the enclosing schists (i.e. quartz, muscovite, biotite, garnet, staurolite, kyanite, fibrolite, andalusite, oligoclase, rutile and ilmenite), but differ in their coarser average grain size and larger proportion of plagioclase, which appears as isolated porphyroblasts, and in plagioclase-rich trondhjemitic layers and diffuse differentiates (García-Casco et al., 1993). Fig. 4 shows the age spectra and isotope correlation plots for muscovite and biotite from this sample. Isochron

dates of 19.1 ± 0.8 Ma and 18.8 ± 0.6 Ma were obtained. Muscovite again displays a relatively scattered release pattern, probably due to incomplete recrystallization and chemical reequilibration of the primary high-pressure micas during subsequent decompression (García-Casco et al., 1993).

Samples T316 and T337 are both leucocratic gneisses from the core of the gneiss complex, bearing simpler assemblages of quartz, plagioclase, K-feldspar, muscovite and biotite ($\pm$apatite, tourmaline, rutile, ilmenite, sillimanite, andalusite, zircon and dumortierite). Reaction textures in these rocks indicate that decomposition of initial very Si-rich muscovites (up to 6.66 atoms
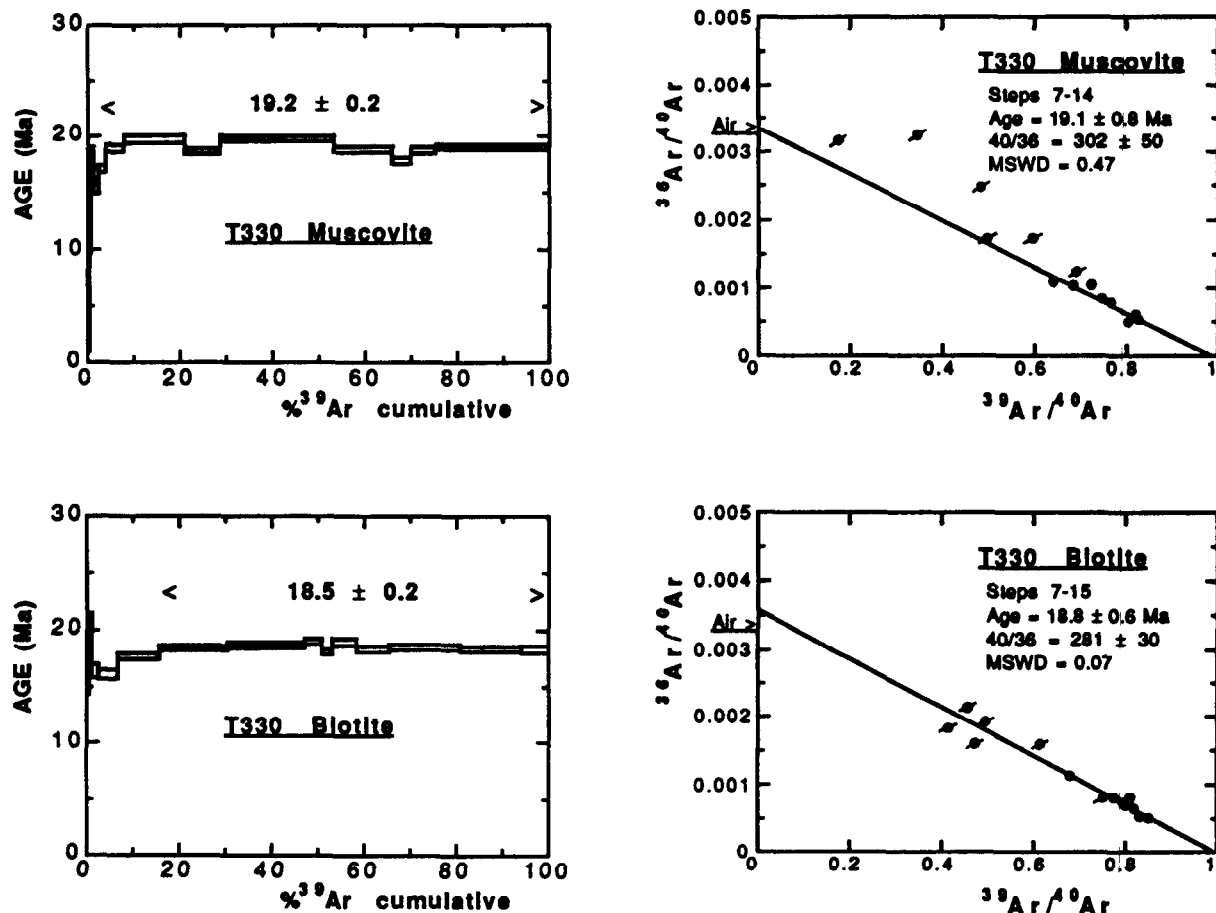

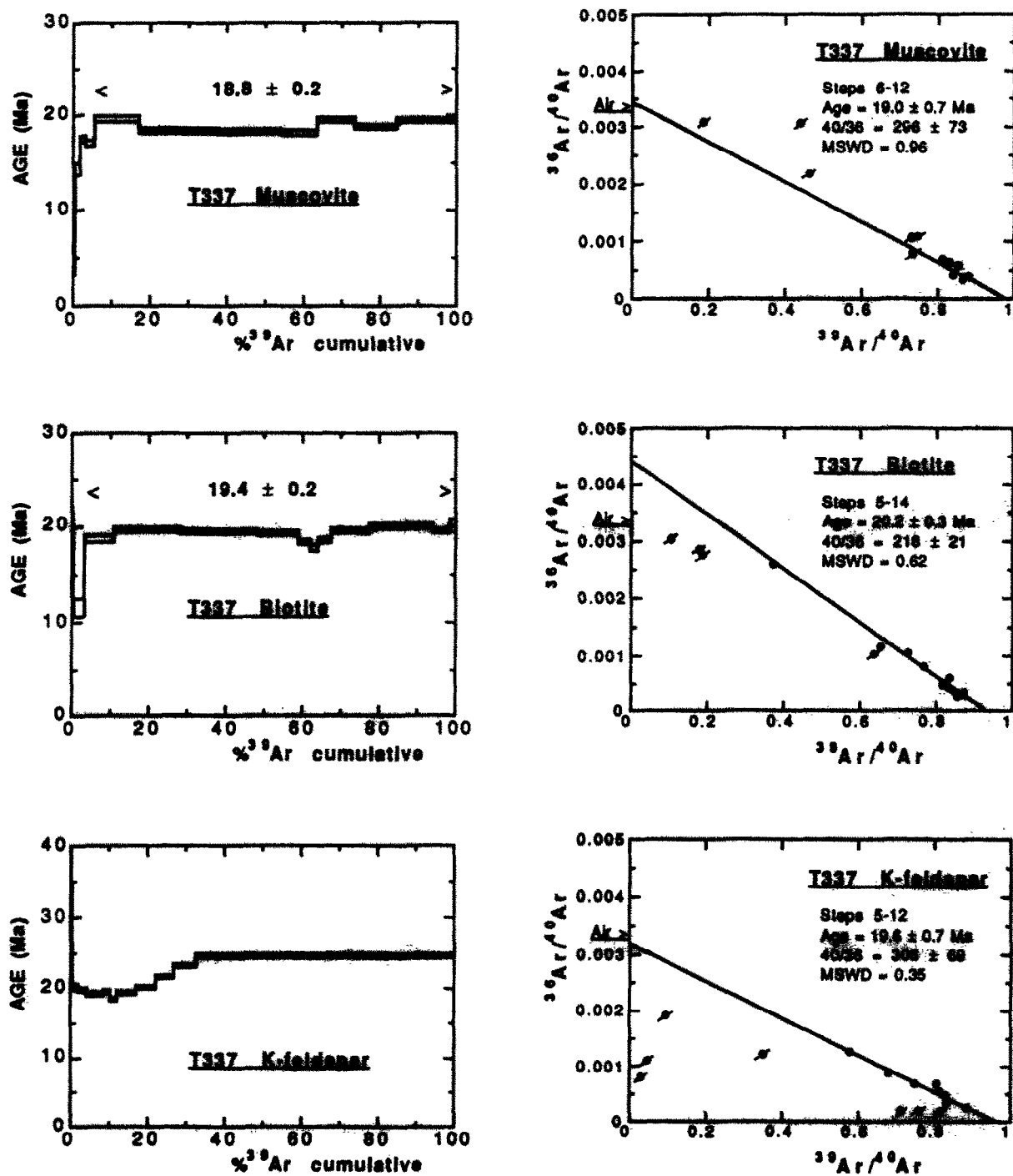Fig. 4. Age spectra and isotope correlation plots from pelitic gneisses of Torrox.

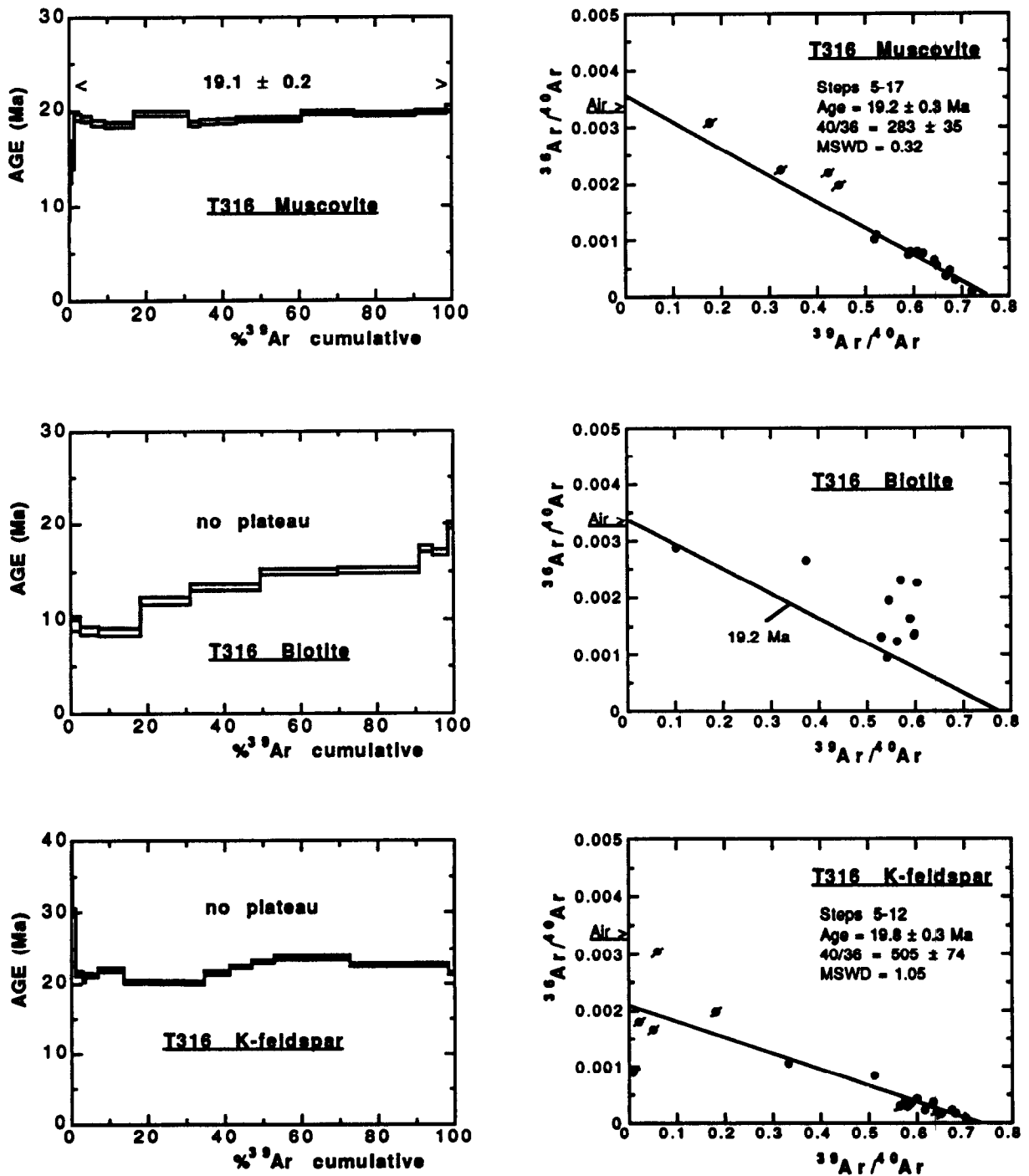Fig. 5. Age spectra and isotope correlation plots from augen gneisses of Torrox.

Fig. 6. Age spectra and isotope correlation plots from banded gneisses of Torrox.

p.f.u. normalized to 20 oxygens and 4 OH) took place in response to fast decompression, contemporaneously with ductile deformation responsible for the main regional deformation (see the $P–T$ path in Fig. 2; García-Casco et al., 1993). For this study, two samples were chosen so as to represent systems in which most muscovite was recrystallized at low pressure (T337) and in which a fair amount of the initial Si-rich muscovite was preserved (T316).

Release age spectra and isochron plots for muscovite, biotite and microcline from sample T337 are shown in Fig. 5. The age spectra for muscovite and biotite are very similar to those reported above and isochron dates of 19.0 ± 0.7 Ma and 20.2 ± 0.3 Ma are indicated. However, for biotite, the initially trapped Ar has an $^{40}Ar/^{36}Ar$ ratio significantly lower than 295.5, making the interpretation of the age intercept ambiguous. Ca/K values for this biotite are low but they demonstrate a systematic correlation between the higher Ca/K ratios and the younger ages. Contamination of biotite by chlorite intergrowths may offer an explanation for the observed isotopic features, and we suspect that the alignment of the data points in the isochron plot is partly fortuitous. The age spectrum from microcline exhibits a discordant pattern. Old ages and high Ca/K values are obtained in the first heating fractions representing about 5% of gas released. Young ages ranging from 20.3 to 18.5 Ma and relatively low Ca/K values are derived from the following 20% of gas released. The corresponding heating steps lie on a single mixing line with an intercept age of 19.6 ± 0.7 Ma and an initial $^{40}Ar/^{36}Ar$ ratio of 306 ± 69. Ages increase over the final 80% of gas released from 21.7 to 24.7 Ma. Unfortunately, the sample has been melted during the last heating increment representing 70% of release. Nevertheless, our interpretation is that the isochron age derived from the low-temperature fractions represents a maximum age for the complete closure of the microcline to Ar diffusion during cooling at low pressure. The minimum age of 18.5 ± 0.2 Ma in the age spectrum is considered the best estimate for closure.

Data on biotite, muscovite and microcline from gneiss T316 are shown in Fig. 6. Muscovite dis-plays the same age pattern and has an isochron date of 19.2 ± 0.3 Ma defined by thirteen heating steps. The age spectrum for biotite is discordant with apparent ages progressively increasing with experimental temperature from about 9 to 20 Ma. Isochron data do not exhibit a linear correlation, whereas Ca/K values are low and constant, suggesting the absence of chlorite contamination in this sample. Microprobe data indicate that this biotite is compositionally heterogeneous, as illustrated by point analyses with Ti contents varying between 0.04 and 0.4, and Mg/Fe ratios between 0.164 and 0.038, again demonstrating that complete metamorphic equilibrium was not reached during the last low-pressure overprinting. We suggest that the age gradient reflects the outgassing of a mixture of micas with different diffusion characteristics related to a compositional effect. Such a compositional effect on argon diffusion in biotite has been documented by Harrison et al. (1985), suggesting that the higher the Mg/Fe ratio the higher the activation energy required for diffusion. Therefore, it seems likely that biotite grains or sub-grains with the lower Mg/Fe mainly contribute to the gas released at low temperature in Fig. 6, whereas those with higher Mg/Fe were preferentially degassed at high temperature. Note that variations in the effective diffusion radius or in the composition of the initially trapped argon could also have played a role. The microcline has an age spectrum reminiscent of that obtained on microcline T337 (Fig. 6). Ages first decrease from a maximum of about 900 Ma to 30 Ma with a concomitant decrease of Ca/K related to 1% of gas released. The next 40% of gas release gives ages ranging from 20.2 to 22.0 Ma with constant Ca/K values. The corresponding isochron age is 19.8 ± 0.3 Ma with a high $^{40}Ar/^{36}Ar$ ratio, suggesting the trapping of excess argon at the time of Ar retention in microcline. Ages related to the final 60% of gas released have an upward-convex evolution with a maximum value of 23.7 Ma and no clear linear relationship in the correlation plot. At present it is difficult to state whether these old ages result from excess Ar contamination or from incomplete resetting of an older (pre-Alpine or Alpine) K-feldspar.

4.2. Serranía de Ronda

In this area, eight samples collected from different levels in the Alpujarride stack shall be described in ascending order.

Sample AA9 is a phlogopite-bearing amphibolite intercalated within Triassic(?) marbles in the southeastern slope of the Sierra Blanca. The rock preserves a high-temperature mylonitic fabric with subhedral hornblende, plagioclase and quartz as the main constituents and no evidence of retrogression. Sample AA24 belongs to the same carbonate sequence of the Blanca unit, to the north of Estepona, and originates from a layer of coarse-grained phlogopite–diopside marble. Phlogopite and amphibole have isochron dates of 20.2 ± 0.3 Ma and 19.1 ± 1.2 Ma, respectively (Fig. 7), very similar to the ages reported from the Vélez Málaga–Sierra Tejeda area.

Samples AA10 and AA11 consist of granodiorite dykes emplaced into a N–S shear zone within the Sierra Alpujata peridotite massif, northeast of Marbella. Both samples bear an assemblage of quartz, K-feldspar, plagioclase, biotite, muscovite, cordierite and sillimanite, suggesting that these rocks derived from anatectic liquids. Except for cordierite, which shows variable alteration to fine micaceous aggregates, the assemblages are well preserved. Sample AA10 bears a strong mylonitic imprint, resulting in the development of quartz ribbons, pressure shadows, rotation of feldspar porphyroclasts in the mylonitic foliation and more pronounced retrogression of cordierite. The age spectrum and isotope correlation plot for biotite AA11 derived from the undeformed granodiorite are shown in Fig. 8. The sample has an isochron date of 19.3 ± 0.2 Ma which is about 1 Ma younger than the biotite age of the mylonitic sample AA10. This latter age is a total gas age derived from a two-step experiment because of the low amount of available material. However, since the two apparent ages of the experiment are statistically identical and since biotites generally yield flat plateaus and concordant isochron dates for a large percentage of gas released, we consider that 20.2 Ma is a true cooling age for biotite AA10. The age difference between AA10 and AA11 samples indicates that, after granite emplacement

and deformation, cooling through 300–350°C occurred earlier along the mylonitic zones than within the massive rock bodies, probably because the sheared zones have been the locus of easier heat dissipation. These ages of 19–20 Ma for anatectic melts intruding the peridotites are consistent with the Rb–Sr whole-rock date of 22 ± 4 Ma determined on a leucocratic dyke in the Bermeja peridotites (Priem et al., 1979), corroborated by U–Pb monazite ages (D. Gebauer, pers. commun.).

Samples AA12, AA15, AA21 and AA22 are all high-grade metapelites from the basement of the Casares–Los Reales units. Samples AA12 and AA22 are coarse-grained granulites representative of the highest-grade crustal rocks in these units, that typically outcrop next to the peridotite bodies. Both samples bear well-preserved high-pressure assemblages (quartz–garnet–K-feldspar–plagioclase–kyanite–rutile). Small biotite grains are also preserved as inclusions in garnet. The low-pressure overprint on these samples is variable (more advanced in sample AA22) and consists of direct inversion of kyanite to sillimanite and the development of spinel–cordierite–biotite–ilmenite coronas and symplectite overgrowths on garnet. The HP assemblage probably equilibrated at/or near 750°C at a minimum pressure of 8–11 kbar (cf. Sect. 2.2). Samples AA15 and AA21 are both high-grade gneisses overlying the granulites, and bearing complex disequilibrium assemblages of quartz, K-feldspar, plagioclase, muscovite, biotite, sillimanite, andalusite, kyanite, garnet and staurolite (more rarely cordierite). Textural development within these rocks indicates strong low-pressure overprinting of an initial high-pressure assemblage (kyanite, garnet and staurolite), as discussed by Torres-Roldán (1981).

The very well-preserved granulitic assemblage in sample AA12 (Sierra Alpujata) contains large garnet with inclusions of prograde biotite while scarce syn-decompressional biotite occurs in the rock matrix, around garnet. Only prograde biotites have been dated with the laser-probe ablation technique (see Maluski and Monié, 1988, for the technical aspect) since it was hoped that the petrographic nature of the host garnet might have

prevented biotite from further argon reequilibration during the low-pressure evolution. Five laser shots, each of 40 μm in diameter and 30 ns in duration, were performed to provide a sufficient volume of argon to be accurately analyzed by the mass spectrometer. Total fusion experiments give ages of 19.1 ± 0.3 Ma, 19.0 ± 0.5 Ma and 16.8 ± 0.4 Ma (Table 1). These ages are in good agreement with those determined up to now in this study, the younger age probably being the result of an imprecise evaluation of the atmospheric contribution (i.e. ^{36}Ar) within these young samples, or of a non-atmospheric composition of the initially trapped argon. Nonetheless, these dates

clearly demonstrate that the prograde biotites included in garnet became closed to argon diffusion at the same time as the low-pressure matrix biotites analyzed in the country rocks. This indicates that radiogenic argon did not accumulate within the biotite inclusions but was able to migrate through the host garnet along cracks or grain boundaries.

Fig. 8 shows the age spectrum and isochron correlation plot for muscovite AA15 from a high-grade pelitic gneiss of the Yunquera unit. Despite the presence of abundant high-pressure relict minerals, the muscovite has an isochron date of 19.5 ± 0.6 Ma that is indistinguishable
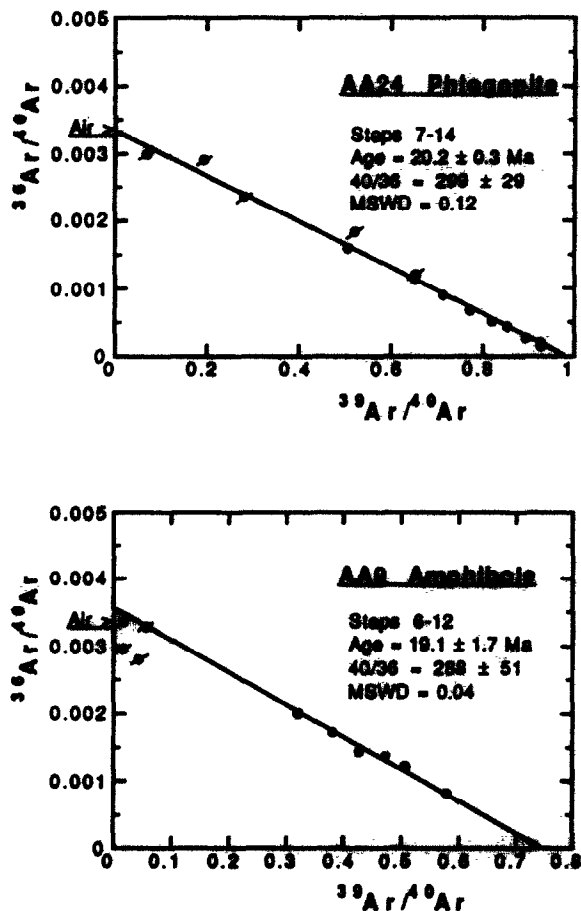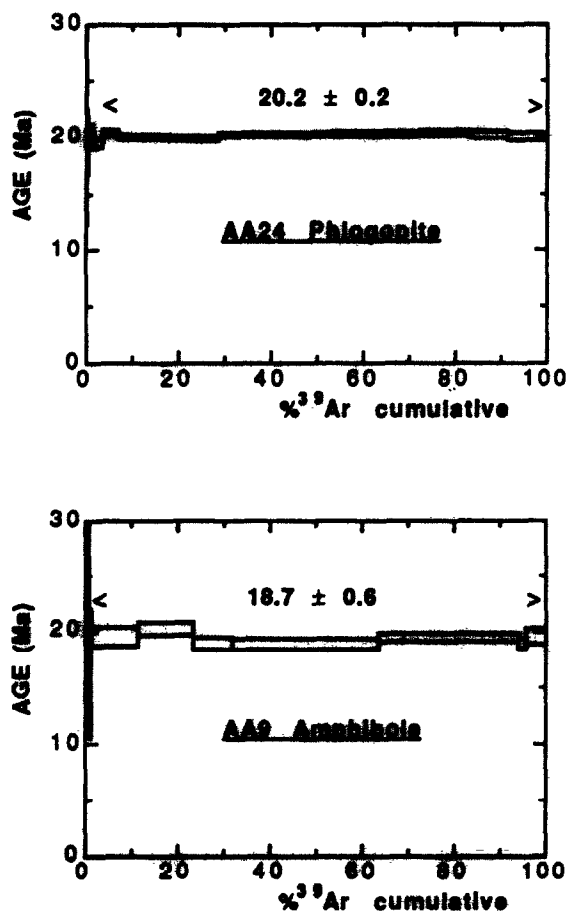

Fig. 7. Age spectra and isotope correlation plots from marbles and amphibolites of the Blanca unit.

from the dates presented above, suggesting the lack of radiogenic argon inherited from the early metamorphic evolution.

Two gneiss and granulite samples were selected in the Casares–Los Reales type locality, to the northwest of the Sierra Bermeja peridotite (Fig. 9). Biotite AA21 from the gneiss has a well-developed plateau date of 21.3 ± 0.3 Ma and a similar isochron date. Biotite AA22 from a granulite adjacent to the peridotites displays statistically similar plateau and isochron ages of 21.6 ± 0.2 Ma. These ages are consistent with two K–Ar biotite ages reported by Loomis (1975) and Priem et al. (1979) from the same area. This would suggest that the Casares–Los Reales unit, i.e. the highest structural unit of the Western

Alpujarrides, cooled through 300–350°C approximately 2 Ma before the deeper, more easterly Alpujarride units. The implications of this diachronous cooling are discussed below.

4.3. Viñuela formation

The Viñuela formation (Boulin et al., 1973) is representative of a number of syn-tectonic sedimentary formations within the Betic–Rif belt whose deposition took place in the Early Miocene, often sealing preexisting nappe contacts (Martín-Algarra, 1987). Of special interest is that the basal breccia contains a variety of metamorphic clasts, many of which can be easily correlated with the graphitic schists that make the bulk of
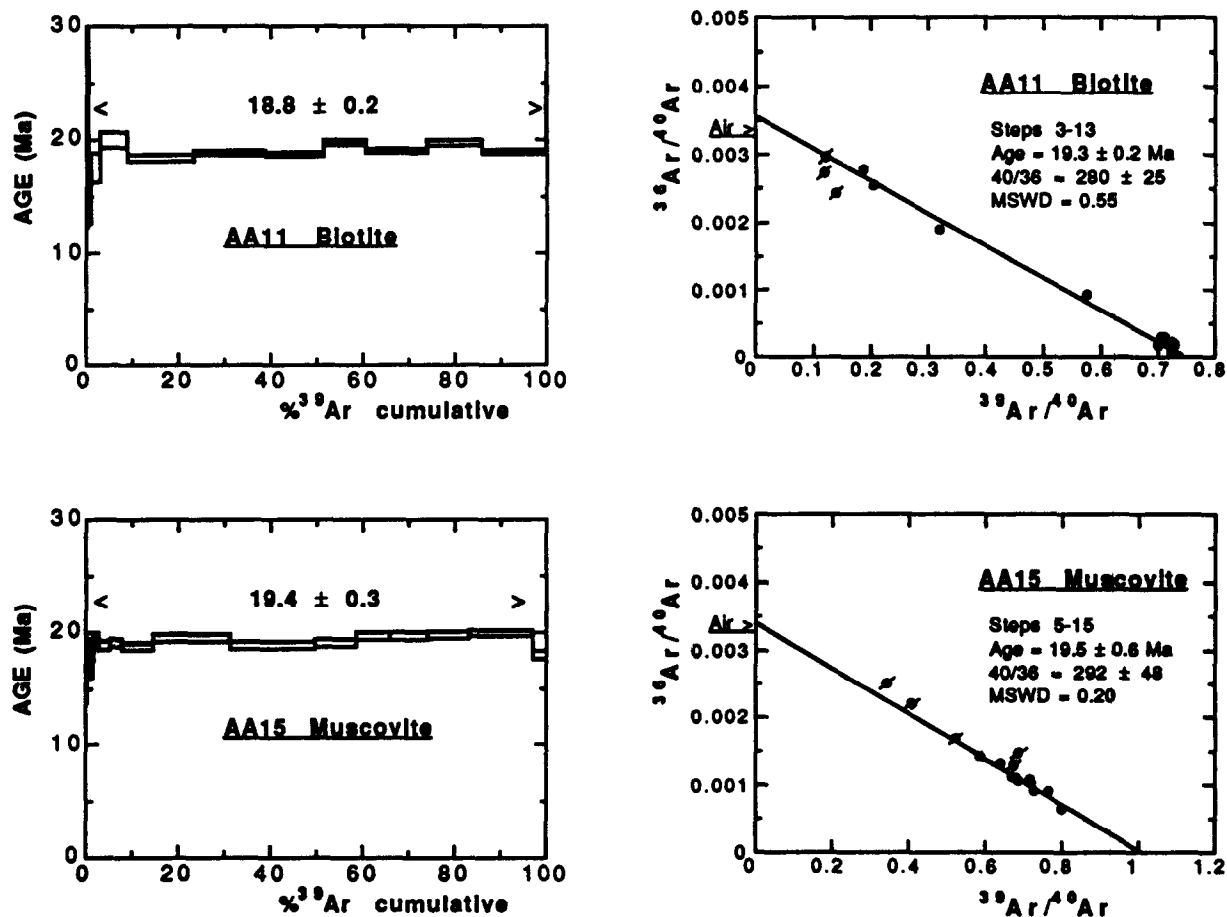

Fig. 8. Age spectra and isotope correlation plots from a cordierite–granite of Ojen and a high-grade pelitic schist of the Yunquera unit.
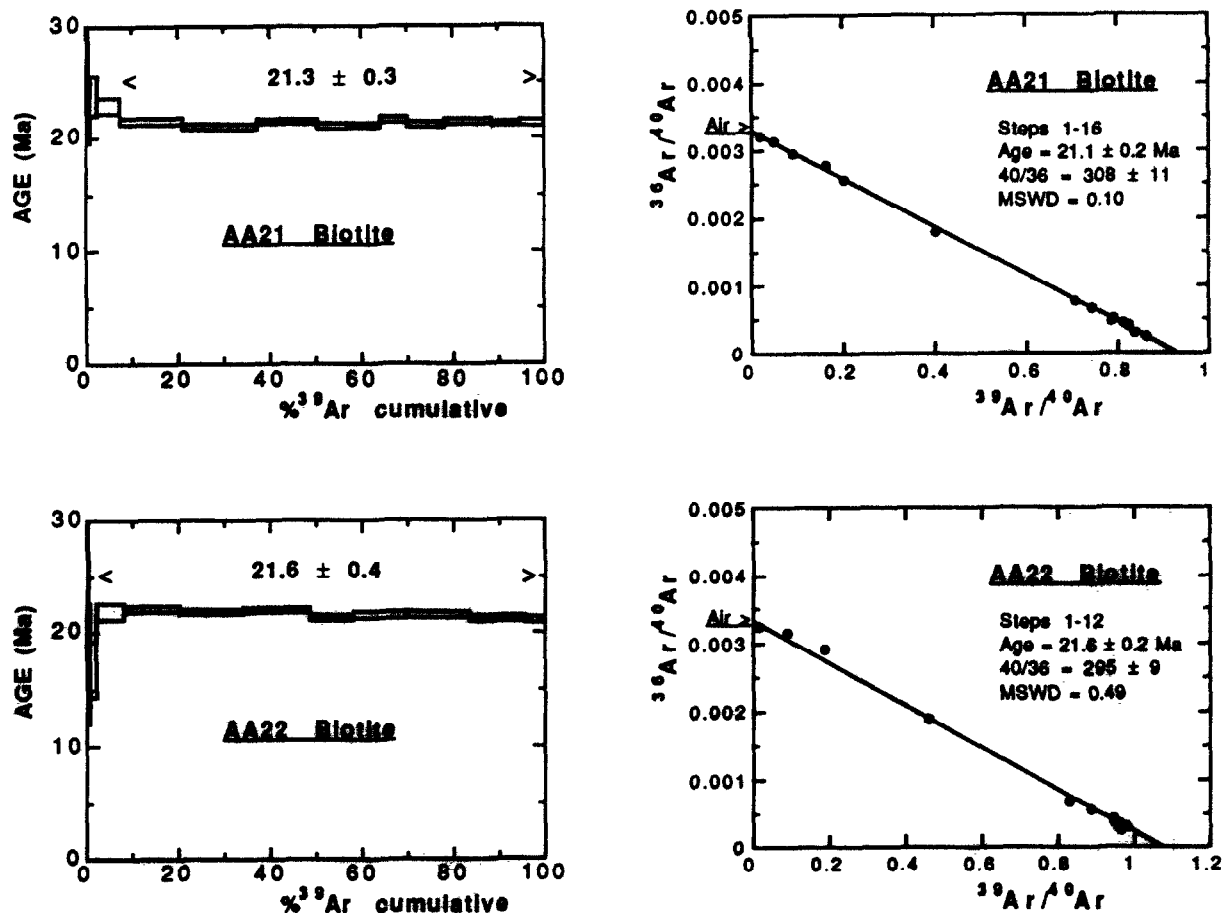
Fig. 9. Age spectra and isotope correlation plots from gneisses and granulites of the Casares–Los Reales type locality.
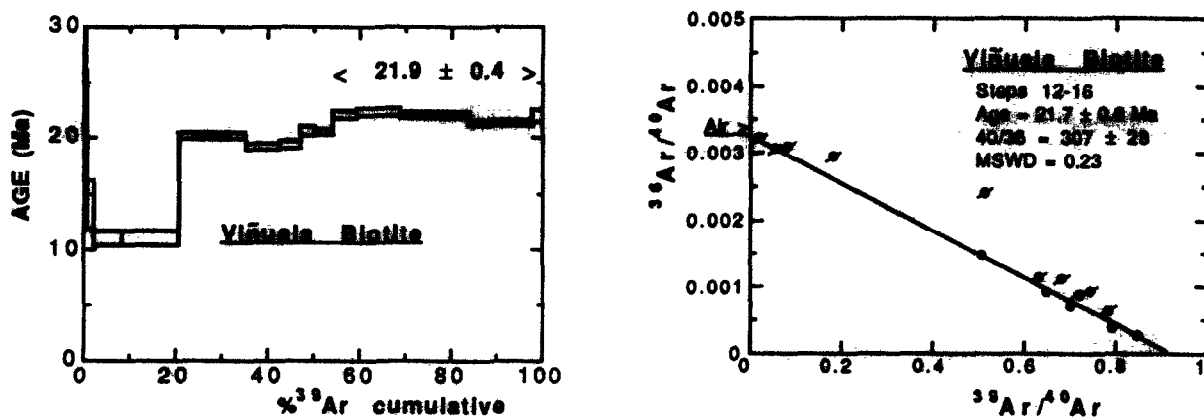

Fig. 10. Age spectrum and isotope correlation plot from a micaschist pebble of the Viñuela formation.

the Palaeozoic basement of the Torrox unit. The deposition of the basal breccia was succeeded by marly deposits containing planktonic Foraminifera indicating an early Burdigalian age (González-Donoso et al., 1982), thus constraining the time of aerial exposure of the Cómpeta–Torrox unit to not later than about 19 Ma (Harland et al., 1990).

Sample VIN02, a graphitic schist with quartz, biotite, muscovite, staurolite, garnet, plagioclase and andalusite, is from a pebble within the basal breccia that was chosen for $^{40}Ar/^{39}Ar$ dating because it showed little evidence of retrogression or alteration. Fig. 10 illustrates the age spectrum and isotope correlation plot for a biotite concentrate of this schist. In the lower temperature increments (450–950°C), discordant ages are recorded, climbing from 11.1 to 20.6 Ma. The final part of the spectrum yields a plateau of 21.9 ± 0.4 Ma over more than 50% of the gas release. A similar intercept age of 21.7 ± 0.6 Ma is derived from the isotope correlation diagram. Ca/K values are low and similar to those obtained on biotites throughout this study. Internal variations in Ca/K during incremental heating

have no direct correlation with the evolution of ages in the spectrum.

The young ages over the first 20% of release probably reflect some interaction with a meteoric phase after the deposition of the Viñuela formation. The date of 21.7 Ma is similar to that obtained on the Casares–Los Reales crustal envelope and can be regarded as the time at which the original graphitic schist cooled below 370°C (cf. Sect. 5), before its surface exposure and incorporation into the Viñuela breccia. This date agrees with the biostratigraphic constraints pointing to an early Burdigalian age for this formation.

5. Discussion

Fig. 11 presents a histogram summarizing more than 40 K–Ar, $^{40}Ar/^{39}Ar$, Rb–Sr and Sm–Nd cooling ages from this and previous studies in the Western Alpujarrides. Despite the polyphase metamorphic history of the Alpujarrides, all closure ages cluster in a narrow range between 23.4 and 15.5 Ma, most of them (~ 30) in the 19–20
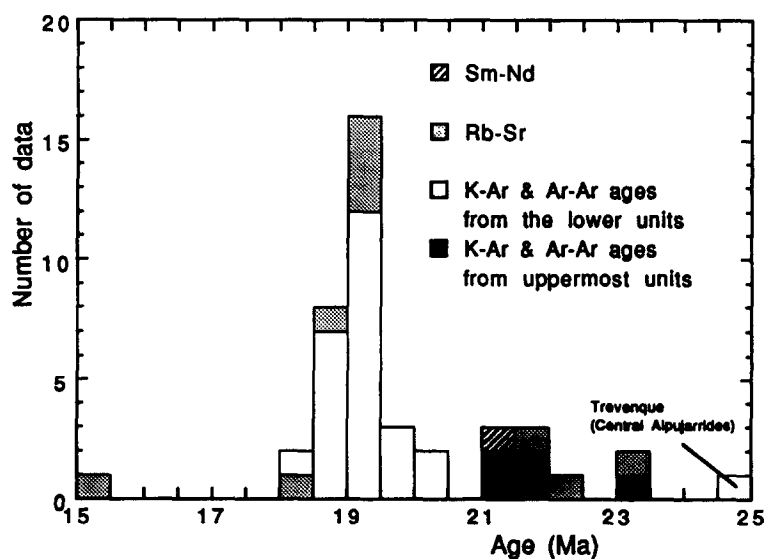

Fig. 11. Arrhenius plot of log (D/a^2) versus reciprocal absolute temperature for samples T316 and T337 of Torrox. The diffusion properties of the smaller domains in the K-feldspars have been calculated by assuming that the diffusion domain geometry is represented by spheres. The activation energy E and effective frequency factor D_0/a^2 return a closure temperature of $304 \pm 33°C$ for the smaller domains, for a cooling rate of 200°C/Ma.

Ma age range. Consequently, the ages of older events in the tectonothermal evolution of the Western Alpujarrides are not constrained by this data set. This homogeneity of results for metamorphic, granitic and peridotitic rocks exposed over nearly 4000 km² in the Western Betic orogen has important implications concerning the cooling and exhumation history of the Alpujarride rocks.

5.1. Cooling rate estimates

The estimation of cooling rates requires knowledge of the closure temperatures for argon in the various minerals dated in this study. The closure temperatures of the different mineral species is not unique as it depends on diffusion grain size, cooling rate and activation energy according to the equations given by Dodson (1973).

Harrison et al. (1985) reported diffusion experiments on biotite Ann_{56} that yielded an activation energy of 47 kcal/mol and a closure temperature of 340°C for an effective diffusion radius of 150 μm and a cooling rate of 100°C/m.y. Studying the effect of grain size on biotite ages by single-grain step-heating laser dating, Wright et al. (1991) suggested a larger diffusion radius of 225 μm. By combining this value with a cooling rate of 200°C/m.y. (see below) and adopting the diffusion parameters of Harrison et al. (1985), we obtain a closure temperature of 370°C for biotites. The data of Giletti (1974) have been used to calculate the closure temperature of phlogopite. Assuming the same diffusion radius and cooling rate as for biotite, we estimate T_c to be 470°C. For muscovite, we assign a closure temperature of 430°C on the basis of the diffusion parameters given by Robbins (1972), for a diffusion radius of 30 μm and a cooling rate of 200°C/m.y. A compositional effect on argon diffusion may also be responsible for a variable closure temperature in the white mica group (Monié and Chopin, 1991; Scaillet et al., 1992). To take this effect into account, an uncertainty of $\pm$ 30°C is attached to the closure temperatures mentioned.

Isothermal–hydrothermal experiments on hornblende (Harrison, 1981) yielded diffusion parameters that return a closure temperature of 550°C for a cooling rate of 200°C/m.y. Laser
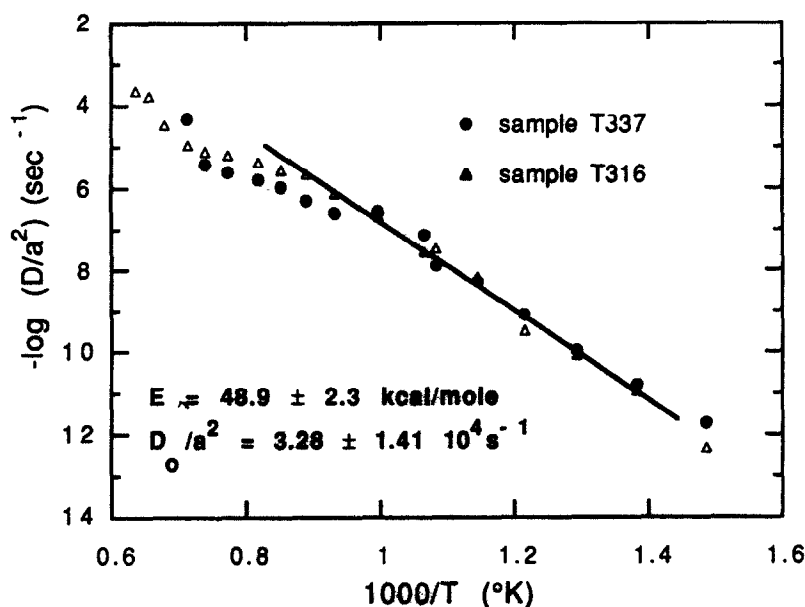

Fig. 12. Histogram of geochronological data in the Western Alpujarrides. Data sources are Loomis (1975), Priem et al. (1979), Zindler et al. (1983), Reisberg et al. (1989), Zeck et al. (1989, 1992), Monié et al. (1991) and this work. Most ages cluster in the range 19–20 Ma, which is suggestive of fast cooling rates.

probe dating of homogeneous hornblende suggests that the effective diffusion radius can occasionally be equal to the grain size (Lee et al., 1990), implying a very high closure temperature of 640°C for a radius of 500 μm and a cooling rate of 200°C/m.y.. Considering the uncertainty about the dimension governing diffusive exchange, we adopt a closure temperature of 600 ± 50°C.

Calculations based on stepwise $^{40}Ar/^{39}Ar$ degassing of K-feldspars in vacuum often yield reliable diffusion parameters using the Arrhenius plot (Berger and York, 1981; Harrison and McDougall, 1982). Moreover, recent work on K-feldspars with discordant age spectra due to slow cooling provides evidence that their degassing behaviour results from the coexistence of discrete domains with different diffusion sizes and activation energies as revealed by the departure from linearity of the diffusion data in the Arrhenius plot (Lovera et al., 1989). Modelling the Arrhenius plot suggests that closure temperatures within the same sample can vary from about 350°C to 150°C. However, cooling rates inferred in this paper do not allow us to interpret the discordant age spectra of K-feldspars T316 and T335 as reflecting progressive closure during slow cooling because the ages derived at high temperature are significantly older than the plateau ages of micas and amphiboles. More likely, the age difference of 3–5 Ma between the low- and high-temperature portions of the age spectra reflects the presence of a component inherited from the pre-Alpine or early Alpine history of the host gneisses. Both age spectra yield similar minimum ages of 18.5–20 Ma and isochron dates of 19.7 ± 0.5 Ma that represent maximum ages for the closure of the domains having the lowest diffusion size. We have used the Arrhenius plot calculated with a spherical geometry model to estimate the minimum closure temperature of the two feldspars (Fig. 12). The two samples have very similar plots, showing a well-defined linear behaviour for the low-temperature steps (< 850°C), followed by a second linear segment with a lower slope up to 1100°C, while the data above the incongruent melting temperature (1150°C) define a last linear segment with the highest slope. Lovera et al. (1989) have shown that the decrease in slope is not due to a structural breakdown of feldspars during experimental heating, but is characteristic of samples containing a distribution
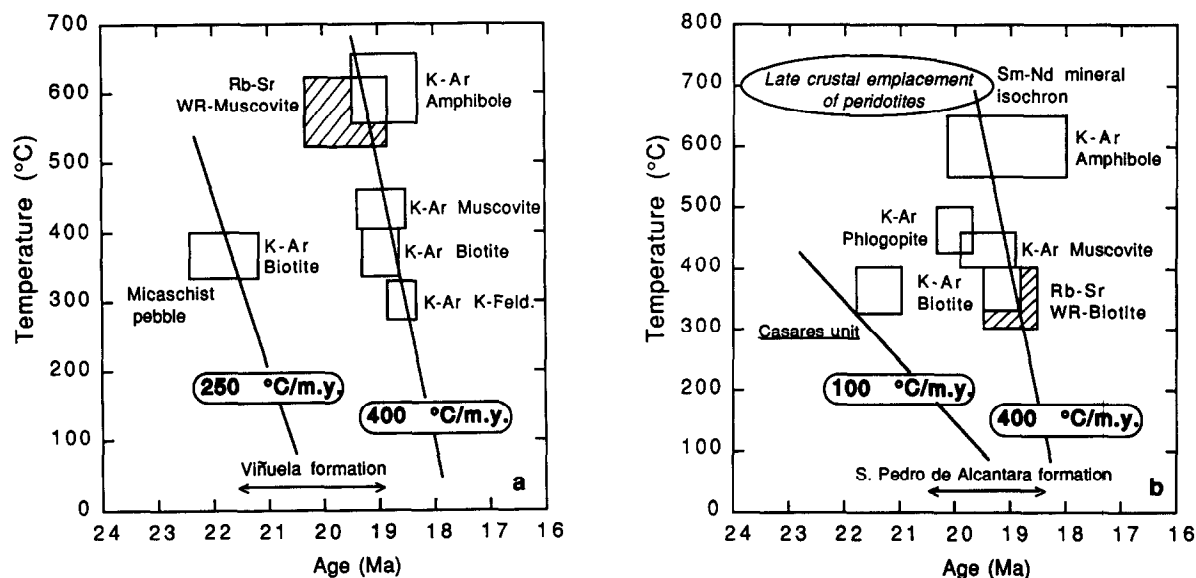

Fig. 13. Temperature–time diagrams for two areas of the Western Alpujarrides constructed from available geochronological data and argon closure temperatures discussed in the text. (a) Vélez Málaga–Sierra Tejeda Massif. (b) Serranía de Ronda.

of diffusion domain sizes. The smaller domains in the sample have an activation energy of 48.9 ± 2.3 kcal/mol with a corresponding D_0/a^2 value of $3.28 \pm 1.41 \times 10^4$ s^{-1}, as calculated from the low-temperature data representing less than 25% of the ^{39}Ar released. These parameters give a closure temperature of $304 \pm 33°C$ for a cooling rate of 200°C/m.y.

Temperature–time diagrams for the Vélez Málaga–Sierra Tejeda and Serranía de Ronda areas are shown in Figs. 13a and 13b, respectively. In Fig. 13a, twelve $^{40}Ar/^{39}Ar$ mineral dates derived from this study and from Monié et al. (1991) and Zeck et al. (1992) constrain the cooling path. These dates have a mean value of 19.0 Ma with a standard deviation of only 0.2 Ma for minerals having closure temperatures ranging from 300 to 600°C. The best defined whole-rock muscovite Rb–Sr age in this area is 19.5 ± 0.7 Ma (Zeck et al., 1989) and has been plotted in the figure with a closure temperature of $575 \pm 50°C$ (Zeck et al., 1992). All these data suggest that the cooling rate was very high in the 19–20 Ma interval and a best-fit line through the data points indicates an average value of 375°C/m.y. ($\pm 210°C$). A cooling line of 400°C/m.y. was drawn in the figure as a reference. Available palaeontological and radiometric data for the transgressive Viñuela formation have also been combined to estimate cooling rates. It is important to note that only minimum values can be deduced since the time at which the rock sample reached the surface and the duration of its surface exposure before incorporation into the Viñuela breccia are unknown data. The minimum cooling rate is 100°C/m.y. assigning a minimum 19 Ma age to the Viñuela formation and a maximum biotite cooling age of 22.3 Ma at 340°C. A 250°C/m.y. cooling line seems to be a reasonable interpretation of the data.

Fourteen $^{40}Ar/^{39}Ar$ and Rb/Sr mineral dates constrain cooling rates in the Serranía de Ronda area (Fig. 13b). These dates have a mean value of 19.3 Ma with a standard deviation of 0.4 Ma despite the large range in closure temperatures. This again suggests fast cooling bracketed between 150 and 400°C/m.y. as indicated by least-square fitting. Note that the biotite dates of the
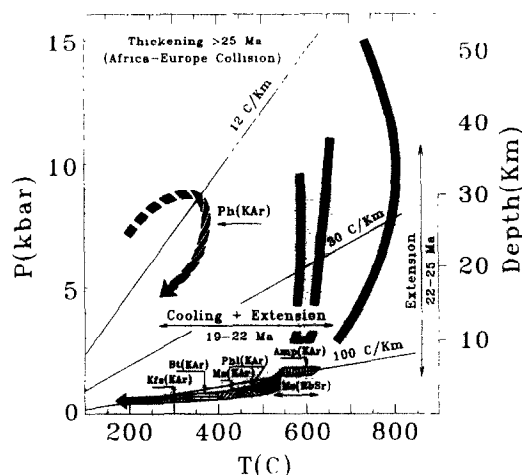

Fig. 14. Projection of geochronological data on synthetic $P-T$ paths of the Western Alpujarrides according to the respective closure temperatures. Different geotherms have been schematized representing: initial conditions (12°C/km) during subduction, crustal thickening and HP/LT metamorphism; possible transient conditions (100°C/km) at the end of the principal phase of decompression; current geotherm in stable continental crust (30°C/km). The figure shows that cooling below 600°C and related blocking of isotopic systems occurred after the main episode of decompression related to the collapse of the previously thickened crust.

Casares–Los Reales unit, northwest of the Sierra Bermeja, are clearly away from the cooling line drawn in Fig. 13b, suggesting an independent cooling history. Unfortunately, assessing a cooling rate for this unit requires more data. A minimum cooling rate of 100°C/m.y. has been calculated on the basis of a minimum age of 18.5 Ma for the nappe-sealing San Pedro de Alcantara formation in this area (Aguado et al., 1990).

The inferred cooling rates through the temperature interval 300–600°C are very high and appear to be uniform across the different units of the study area. Within a normal continental temperature–depth gradient of 30°C/km, cooling rates in the range 100–350°C/m.y. would imply apparent exhumation rates of 3–12 km/m.y. However, the combined $P-T$ and $^{40}Ar/^{39}Ar$ data reported in Fig. 14 suggest that near-isobaric cooling during the 19–20 Ma time interval followed near-isothermal decompression, indicative

of a transition in thermal regime from an extremely steep geothermal gradient (related to regional extension) toward a shallower, more stable geotherm. Accordingly, it is probable that the cooling history of the Western Alpujarrides partly reflects the effects of thermal relaxation from an abnormally steep geotherm to a much lower geotherm over a short interval of time and that exhumation rates were lower than those inferred above. For example, relaxation from a 100°C/km geotherm to a more stable 30°C/km geotherm over a million-year period would cause rocks at 7 km depth to cool from 700°C to 200°C without any additional unroofing at all (England and Jackson, 1987). That no exhumation (tectonic or even erosional) occurred during cooling is nonetheless incompatible with the age constraints obtained on the Viñuela formation that indicate that some rocks attained the surface soon after their cooling through blocking temperature. We suggest that 1–3 km/m.y. represents a possible constraint for exhumation rates in the Western Alpujarrides during the main phase of cooling.

These estimates do not apply to the principal phase of exhumation of these rocks, since the bulk of exhumation occurred before the rocks began passing through the closure temperatures of the minerals dated in this study. Although not constrained by the age data presented in this paper, much higher exhumation rates must have prevailed during this phase as indicated by the near-isothermal decompression trajectories followed (Fig. 14). A minimum $^{40}Ar/^{39}Ar$ age of 24.8 ± 0.4 Ma obtained on a Si-rich phengite from low-grade Triassic metapelites to the east of the area studied may date the end of crustal thickening (i.e. the beginning of decompression; Monié et al., 1991). Since the end of the near-isothermal decompression is estimated at about 22 Ma (i.e., Sect. 2.3), extrapolating this date to higher-grade rocks would suggest average exhumation rates up to 10 km/m.y. for this period. Such very high rates are consistent with the preservation of aragonite in low-grade rocks (Goffé et al., 1989) as well as with evidence for strong overstepping of reaction boundaries during decompression in high-grade gneisses of the Torrox unit (García-Casco et al., 1993).

5.2. The Western Alpujarrides: a "collapsed" terrane

The Western Alpujarrides consist of several stacked units differentiated on the basis of their lithology, metamorphism and mutual structural relationships. However, the present data, which reflect a large range of closure temperatures (see above), suggest that all these units shared an almost uniform fast cooling history at 19–20 Ma, with the exception of the western Casares–Los Reales unit and metamorphic clasts of the Viñuela formation, which cooled ca. 2 Ma earlier. Possible explanations for this behaviour are discussed here, which suggest that the Western Alpujarrides display the characteristics expected of a "collapsed" terrane, related to strikingly fast extensional tectonic development at the end of the Alpine orogeny.

Based on existing petrologic evidence, the Alpujarride metamorphic rocks experienced a simple clockwise P–T path characterized by (a) an early HP/HT stage, (b) near-isothermal decompression, and (c) near-isobaric cooling at low pressure (Fig. 14). As discussed earlier, exhumation during stage (b) was a fast rate process, which points towards gravitational collapse of the previously thickened lithosphere as the most feasible mechanism driving extension. Collapse could have been triggered by the detachment of previously subducted lithosphere beneath the Alboran Sea (Torres-Roldán et al., 1986), and/or by the delamination of a cold root of mantle in the same location (Platt and Vissers, 1989). One main effect of this early extension was to produce an unstable, extremely steep geothermal gradient, which was rapidly followed by thermal relaxation towards a more stable geotherm compatible with the change in tectonic regime. Fast thermal relaxation was achieved through a combination of processes, among which distributed ductile thinning and extensional detachments played significant roles. Extensional detachments had the effect of juxtaposing hot, deep crustal rocks against colder, more superficial units and, as exemplified by our results on the Viñuela formation, this mechanism probably caused the somewhat earlier cooling and eventual exposure of the uppermost

units immediately beneath the Malaguides, prior to their erosion and redeposition as metamorphic clasts in the Late Oligocene–Early Miocene nappe-sealing formations throughout the Gibraltar arc (Feinberg et al., 1990). Similarly, earlier cooling in the deeper, high-grade rocks of the Casares–Los Reales unit (samples AA21 and AA22) may reflect their proximity to the Gibraltar arc (extension-related) thrust that brought the western, hot margin of the Alboran domain over the non-metamorphic Flysch Through, South Iberian and Maghrebian domains in the Early Miocene (García-Dueñas et al., 1992; Torné et al., 1992).

As a whole and compared to "standard" metamorphic belts, the $P–T–t$ path and structural data presented above suggest that the tectono-metamorphic evolution of the Western Alpujarrides after collision might be appropriately regarded as characteristic of a "collapsed" terrane, with:

(a) Early, high-temperature development of extensional structures at all scales, including shear zones and foliation.

(b) Very fast exhumation (in the range of several km/m.y.), leading to a temporary steep geotherm. Generalized, but often incomplete, reequilibration of metamorphic assemblages at low pressure takes place in response to fast decompression along nearly isothermal paths. Exhumation occurred mainly through tectonic denudation (distributed thinning and extensional detachments) and little erosion.

(c) Fast cooling (in the range of several hundred degrees per million years) immediately following exhumation, resulting in a striking convergence of geochronological data. Fast cooling prevents complete low-pressure metamorphic reequilibration, even in high-grade rocks, allowing the preservation of strong disequilibrium relationships.

Collapsed terranes require considerable lithospheric thickening prior to final collapse, and as such they would represent indicators of past continental collision zones. Systematic reconstruction of $P–T–t$ paths in such terranes would be of valuable interest for constraining the kinetics of

processes by which a thickened lithosphere recovers a stable configuration.

References

Aguado, R., Feinberg, H., Durand-Delga, M., Martín-Algarra, A., Esteras, M. and Didon, J., 1990. Nuevos datos sobre la edad de formaciones miocenas transgresivas sobre la Zonas Internas béticas: la formacion de San Pedro de Alcantara (Prov. de Malaga). Rev. Soc. Geol. Esp., 3: 79–85

Azañón, J.M. and Goffé, B., 1991. New occurrence of carpholite–kyanite–cookeite assemblages in the Alpujarrides nappes, Betic Cordilleras, SE Spain. EUG VI Strasbourg, Terra Abstr., 3: 88.

Bakker, H.E., De Jong, K., Helmers, H. and Biermann, C., 1989. The geodynamic evolution of the Internal Zone of the Betic Cordilleras (south-east Spain): a model based on structural analysis and geothermobarometry. J. Metamorph. Geol., 7: 359–381.

Balanyá, J.C. and García-Dueñas, V., 1991. Estructuración de los mantos alpujárrides al W de Málaga (Béticas, Andalucía). Geogaceta, 9: 30–33.

Berger, G.W. and York, D., 1981. Geothermometry from $^{40}Ar/^{39}Ar$ dating experiments. Geochim. Cosmochim. Acta, 45: 795–812.

Boettcher, A.L. and Wyllie, P.J., 1988. Revision of the calcite–aragonite transition, with the location of a triple point between calcite I, calcite II and aragonite. Nature, 213: 792–793.

Bohlen, S.R., Wall, V.J. and Boettcher, A.L., 1983. Experimental investigations and geological applications of equilibrium in the system $FeO–TiO_2–Al_2O_3–SiO_2–H_2O$. Am. Mineral., 68: 1049–1058.

Bonini, W.E., Loomis, T.P. and Robertson, J.D., 1973. Gravity anomalies, ultramafic intrusions, and the tectonics of the region around the Strait of Gibraltar. J. Geophys. Res., 78: 1372–1382.

Boulin, J., Bourgois, J., Chauve, P., Durand-Delga, M., Magne, J., Mathis, V., Peyre, Y., Rivière, M. and Vera, A., 1973. Age Miocène inférieur de la Formation de la Viñuela, discordante sur les nappes internes bétiques (Province de Málaga, Espagne). C.R. Acad. Sci. Paris, 276: 1245–1248.

Coward, M. and Dietrich, D., 1989. Alpine tectonics—an overview. In: M.P. Coward, D. Dietrich and R.G. Park (Editors), Alpine Tectonics. Geol. Soc. Spec. Publ., 45: 1–29.

De Jong, K., Wijbrans, J.R. and Féraud, G., 1992. Repeated thermal resetting of phengites in the Mulhacen Complex (Betic Zone, southeastern Spain) shown by $^{40}Ar/^{39}Ar$ step heating and single grain laser probe dating. Earth Planet. Sci. Lett., 110: 173–191.

Diaz de Federico, A., Torres-Roldán, R.L. and Puga, E., 1990. The rock-series of the Betic substratum. Doc. Trav. I.A.G.M., 12–13: 19–29.

Doblas, M. and Oyarzun, R., 1990. "Mantle core complexes" and Neogene extensional detachment tectonics in the western Betic Cordilleras, Spain: an alternative model for the emplacement of the Ronda peridotites. Earth Planet. Sci. Lett., 93: 76–84.

Dodson, M.H., 1973. Closure temperature in cooling geochronological and petrological systems. Contrib. Mineral. Petrol., 40: 259–574.

England, Ph. and Jackson, J., 1987. Migration of the seismic–aseismic transition during uniform and non-uniform extension of the continental lithosphere. Geology, 15: 291–294.

Feinberg, H., Maate, A., Bouhdadi, S., Durand-Delga, M., Maate, M., Magné, J. and Olivier, P., 1990. Signification des dépôts de l'Oligocène supérieur–Miocène inférieur du Rif interne (Maroc), dans l'évolution géodynamique de l'arc de Gibraltar. C.R. Acad.Sci., Paris, 310: 1487–1495.

Fleck, R.J., Sutter, J.F. and Elliot, D.H., 1977. Interpretation of discordant $^{40}Ar/^{39}Ar$ age spectra of Mesozoic tholeiites from Antarctica. Geochim. Cosmochim. Acta, 41: 15–32.

Fontboté, J.M. and Vera, J.A., 1986. La Cordillera Bética. In: J.A. Comba (Editor), Geología de España. Inst. Geol. Min. Esp., 2: 205–343.

García-Casco, A., Haissen, F. and Torres-Roldán, R.L., 1992. Termobaraometría en metapelitas de grado medio de unitas alpujárrides de la Zona Bética occidental, España. III Congr. Geol. Esp., Salamanca, 1: 338–342.

García-Casco, A., Sánchez-Navas, A. and Torres-Roldán, R.L., 1993. Disequilibrium decomposition and breakdown of muscovite in HP–HT gneisses, Betic alpine Belt (Southern Spain). Am. Mineral., 78, 1130–1148.

García-Dueñas, V. and Balanyá, J.C., 1991. Fallas normales de bajo angulo a gran escala en las Beticas occidentales. Geogaceta, 9: 29–33.

García-Dueñas, V., Balanyá, J.C. and Martínez-Martínez, J.M., 1992. Miocene extensional detachments in the outcropping basement of the northern Alboran Basin (Betics) and their tectonic implications. Geo-Mar. Lett., 12: 88–95.

Giletti, B.J., 1974. Studies in diffusion, I. Argon in phlogopite mica. In: A.W. Hofmann et al. (Editors), Geochemical Transport and Kinetics. Carnegie Institute, Washington, pp. 107–115.

Goffé, B., Michard, A., García-Dueñas, V., González-Lodeiro, F., Monié, P., Campos, J., Galindo-Zaldívar, J., Jabaloy, A., Martínez-Martínez, J.M. and Simancas, J.F., 1989. First evidence of high-pressure, low-temperature meta-

morphism in the Alpujarride nappes, Betic Cordilleras (SE Spain). Eur. J. Mineral., 1: 139–142.

Gómez-Pugnaire, M.T. and Fernández-Soler, J.M., 1987. High-pressure metamorphism in metabasites from the Betic Cordilleras (SE Spain) and its evolution during the Alpine orogeny. Contrib. Mineral. Petrol., 95: 231–244.

González-Donoso, J.M., Linares, D., Molina, E., Serrano, F. and Vera, J.A., 1982. Sobre la edad de formacion de la Viñuela (Cordilleras Beticas, Provincia de Málaga). Real Soc. Esp. Hist. Nat. Bol., 80: 255–275.

Harland, W.B., Armstrong, R.L., Cox, A.V., Craig, L.E., Smith, A.G. and Smith, D.G., 1990. A geologic time scale 1989. Cambridge Univ. Press, Cambridge, 263 pp.

Harrison, T.M., 1981. Diffusion of ^{40}Ar in hornblende. Contrib. Mineral. Petrol., 78: 324–331.

Harrison, T.M. and McDougall, I., 1982. The thermal significance of potassium feldspars K/Ar ages inferred from $^{40}Ar/^{39}Ar$ age spectrum results. Geochim. Cosmochim. Acta, 46: 1811–1820.

Harrison, T.M., Duncan, I. and McDougall, I., 1985. Diffusion of ^{40}Ar in biotite: temperature, pressure and compositional effects. Geochim. Cosmochim. Acta, 49: 2461–2468.

Heizler, M.T. and Harrison, T.M., 1988. Multiple trapped argon isotope components revealed by $^{40}Ar-^{39}Ar$ isochron analysis. Geochim. Cosmochim. Acta, 52: 1295–1303.

Holdaway, M.J., 1971. Stability of andalusite and the aluminium–silicate diagram. Am. J. Sci., 271: 97–131.

Hurford, A.J., Flisch, M. and Jäger, E., 1989. Unravelling the thermo-tectonic evolution of the Alps: a contribution from fission track analysis and mica dating. In: M.P. Coward, D. Dietrich and R.G. Park (Editors), Alpine Tectonics. Geol. Soc. Spec. Publ., 45: 369–398.

Kornprobst, J., 1974. Contribution à l'étude pétrographique et structurale de la zone interne du Rif (Maroc septentrional). Serv. Géol. Maroc Mem., 25, 249 pp.

Lee, J.K.W., Onstott, T.C. and Hanes, J.A., 1990. An $^{40}Ar/^{39}Ar$ investigation of the contact effects of a dyke intrusion, Kapuskasing Structural Zone, Ontario. A comparison of laser microprobe and furnace extraction techniques. Contrib. Mineral. Petrol., 105: 87–105.

Loomis, T.P., 1972. Contact metamorphism of pelitic rocks by the Ronda ultramafic intrusion, southern Spain. Geol. Soc. Am. Bull., 83: 2449–2474.

Loomis, T.P., 1975. Tertiary mantle diapirism, orogeny and plate tectonics east of the Strait of Gibraltar. Am. J. Sci., 275: 1–30.

Loomis, T.P., 1976. Irreversible reactions in high-grade metapelitic rocks. J. Petrol., 17: 559–588.

Lovera, O.M., Richter, F.M. and Harrison, T.M., 1989. $^{40}Ar/^{39}Ar$ thermochronology for slowly cooled samples having a distribution of diffusion domain size. J. Geophys. Res., 94: 17917–17935.

Mäkel, G.H., 1985. The geology of the Malaguide complex and its bearing on the geodynamic evolution of the Betic–Rif orogen (southern Spain and northern Morocco). Geol. GUA Pap., 22, 263 pp.

Maluski, H. and Monié, P., 1988. $^{40}Ar-^{39}Ar$ laser-probe

multi-dating inside single biotites of a Variscan or-
thogneiss (Pinet Massif Central, France). Chem. Geol.
(Isot. Geosci. Sect.), 73: 245–263.

Martín-Algarra, A., 1987. Evolución Geológica Alpina del
contacto entre las zonas Internas y las zonas Externas de
la Cordillera Bética (Sector Occidental). Doct. thesis,
Granada Univ., 1368 pp.

McDougall, I. and Harrison, T.M., 1988. Geochronology and
thermochronology by the $^{40}Ar/^{39}Ar$ method. Clarendon
Press, Oxford, 212 pp.

Michard, A., Chalouan, A., Montigny, R. and Ouazzani-
Touhami, M., 1983. Les nappes cristallophylliennes du Rif
(Sebtides, Maroc), témoins d'un édifice alpin de type pen-
nique incluant le manteau supérieur. C.R. Acad. Sci.,
Paris, 296: 1337–1340.

Michard, A., Goffé, B., Chalouan, A. and Saddiqi, O., 1991.
Les corrélations entre les Chaines bético–rifaines et les
Alpes et leurs conséquences. Bull. Soc. Géol. Fr., 162:
1151–1160.

Monié, P. and Chopin, C., 1991. $^{40}Ar/^{39}Ar$ dating in coesite-
bearing and associated units of the Dora Maira massif,
Western Alps. Eur. J. Mineral., 3: 239–262.

Monié, P., Galindo-Zaldívar J., González-Lodeiro F., Goffé,
B. and Jabaloy, A., 1991. $^{40}Ar/^{39}Ar$ geochronology of
Alpine tectonics in the Betic Cordilleras (southern Spain).
J. Geol. Soc. London, 148: 289–297.

Newton, R.C. and Kennedy, G.C., 1968. Jadeite, analcite,
nepheline and albite at high temperature and pressure.
Am. J. Sci., 266: 728–735.

Nijhuis, H.J., 1964. Plurifacial Alpine Metamorphism in the
South-Eastern Sierra de los Filabres (SE Spain). Thesis,
Amsterdam Univ., 151 pp.

Obata, M., 1980. The Ronda peridotite: garnet-, spinel-, and
plagioclase-lherzolite facies and the $P-T$ trajectories of a
high-temperature mantle intrusion. J. Petrol., 21: 533–572.

Pearson, D.G., Davies, G.R. and Nixon, P.H., 1993. Geo-
chemical constraints on the petrogenesis of diamond facies
pyroxenites from the Beni Bousera peridotite massif, N
Morocco. J. Petrol., 34: 125–172.

Platt, J.P. and Vissers, R.L.M., 1989. Extensional collapse of
thickened continental lithosphere: a working hypothesis
for the Alboran Sea and Gibraltar arc. Geology, 17: 540–
543.

Priem, H.N.A., Boelrijk, N.A.I.M., Hebeda, E.H., Oen, I.S.,
Verdurmen, E.A.T. and Verschure, R.H., 1979. Isotopic
dating of the emplacement of the Ronda ultramafic masses
in the Serrania de Ronda, Southern Spain. Contrib. Min-
eral. Petrol., 70: 103–109.

Puga, E., 1977. Sur l'existence dans le complexe de la Sierra
Nevada (Cordillères Bétiques, Espagne du Sud) d'éclogites
et sur leur origine probable à partir d'une croûte océanique
mésozoïque. C.R. Acad. Sci., Paris, 285: 1379–1382.

Puga, E., Diaz de Federico, A., Fediukova, E., Bondi, M. and
Morten, L., 1989. Petrology, geochemistry and metamor-
phic evolution of the ophiolitic eclogites and related rocks
from the Sierra Nevada (Betic Cordilleras, Southeastern
Spain). Schweiz. Mineral. Petrogr. Mitt., 69: 435–445.

Reisberg, L., Zindler, A. and Jagoutz, E., 1989. Further Sr
and Nd isotopic results from peridotites of the Ronda
Ultramafic Complex. Earth Planet. Sci. Lett., 96: 161–180.

Robbins, G.A., 1972. Radiogenic Argon Diffusion in Mus-
covite under Hydrothermal Conditions. M.S. thesis, Brown
University, Rhode Island, 42 pp.

Roddick, J.C., Cliff, R.A. and Rex, D.C., 1980. The evolution
of excess argon in Alpine biotites—a $^{40}Ar-^{39}Ar$ analysis.
Earth Planet. Sci. Lett., 48: 185–208.

Saddiqi, O., Reuber, I. and Michard, A., 1988. Sur la tec-
tonique de dénudation du manteau infracontinental dans
les Beni Bousera, Rif septentrional, Maroc. C.R. Acad.
Sci., Paris, 307: 657–662.

Scaillet, S., Féraud G., Ballèvre, M. and Amouric, M., 1992.
Mg/Fe and [(Mg, Fe)Si–Al₂] compositional control on Ar
behaviour in high-pressure white micas. A $^{40}Ar/^{39}Ar$ con-
tinuous laser-probe study from the Dora–Maira nappe of
the internal western Alps, Italy. Geochim. Cosmochim.
Acta, 56: 2851–2872.

Seideman, D.E., 1976. An $^{40}Ar/^{39}Ar$ age spectrum for a
cordierite-bearing rock: isolating the effect of excess radio-
genic ^{40}Ar. Earth Planet. Sci. Lett., 33: 268–272.

Steiger, R.H. and Jäger, E., 1977. Subcommission on geo-
chronology: convention on the use of decay constants in
geo- and cosmochronology. Earth Planet. Sci. Lett., 36:
359–362.

Thompson, A.B., 1982. Dehydration melting of pelitic rocks
and the generation of H_2O-undersaturated granitic liq-
uids. Am. J. Sci., 282: 1567–1595.

Torné, M., Banda, E., García-Duenas, V. and Balanyá, J.C.,
1992. Mantle–lithosphere bodies in the Alboran crustal
domain (Ronda peridotites, Betic–Rif orogenic belt). Earth
Planet. Sci. Lett., 110: 163–171.

Torres-Roldán, R.L., 1979. The tectonic subdivision of the
Betic zone (Betic Cordilleras, Southern Spain): its signifi-
cance and one possible geotectonic scenario for the west-
ernmost Alpine belt. Am. J. Sci., 279: 19–51.

Torres-Roldán, R.L., 1981. Plurifacial metamorphic evolution
of the Sierra Bermeja peridotite aureole (southern Spain).
Estud. Geol., 37: 115–133.

Torres-Roldán, R.L., Poli, R. and Peccerillo, A., 1986. An
Early Miocene arc–tholeitic dike event from the Alboran
sea: evidence for precollisional subduction and back-arc
crustal extension in the westernmost Mediterranean. Geol.
Rundsch., 75: 219–234.

Tubía, J.M. and Cuevas, J., 1986. High-temperature emplace-
ment of the Los Reales peridotite nappe (Betic Cordillera,
Spain). J. Struct. Geol., 8: 473–482.

Tubía, J.M. and Gil Ibarguchi, J.I., 1991. Eclogites of the
Ojen nappes: a record of subduction in the Alpujarride
complex (Betic Cordilleras, southern Spain). J. Geol. Soc.
London, 148: 801–804.

Tubía, J.M., Cuevas, J., Navarro-Vila, F., Alvarez, F. and
Aldaya F., 1992. Tectonic evolution of the Alpujarride
Complex (Betic Cordillera, southern Spain). J. Struct.
Geol., 14: 193–203.

Van der Wal, D., 1993. Deformation Processes in Mantle

Peridotites with Special Emphasis on the Ronda Peridotite of SW Spain. Thesis, Utrecht Univ. Mem., 102, 180 pp.

Westerhof, A.B., 1977. On the contact relations of high-temperature peridotites in the Serranía de Ronda, southern Spain. Tectonophysics, 39: 579–591.

Wright, N., Layer, P.W. and York, D., 1991. New insights into thermal history from single grain $^{40}Ar/^{39}Ar$ analysis of biotite. Earth Planet. Sci. Lett., 104: 70–79.

York, D., 1969. Least-square fitting of a straight line with correlated errors. Earth Planet. Sci. Lett., 5: 320–324.

Zeck, H.P., Hansen, B.T., Torres-Roldán, R.L., García-Casco, A. and Martín-Algarra, A., 1989. A 21 ± 2 Ma age for the termination of the ductile Alpine deformation in the internal zone of the Betic Cordilleras, South Spain. Tectonophysics, 169: 215–220.

Zeck, H.P., Monié, P., Villa, I.M. and Hansen, B.T., 1992. High rates of cooling and uplift in the Betic Cordilleras, S. Spain. Alpine lithospheric slab detachment, mantle diapirism and extensional tectonics. Geology, 20: 79–82.

Zindler, A., Staudigel, H., Hart, S.R., Endres, R. and Goldstein, S., 1983. Nd and Sr isotopic study of a mafic layer from Ronda ultramafic complex. Nature, 304: 226–230.